

~~RESTRICTED~~~~CLASSIFICATION CANCELLED~~

MAY 7 1945

NATIONAL ADVISORY COMMITTEE FOR AERONAUTICS

TECHNICAL NOTE

No. 968

THE INWARD BULGE TYPE BUCKLING OF MONOCOQUE CYLINDERS

III - REVISED THEORY WHICH CONSIDERS

THE SHEAR STRAIN ENERGY

By N. J. Hoff and Bertram Klein
Polytechnic Institute of Brooklyn



Washington
April 1945

CLASSIFIED DOCUMENT

This document contains classified information affecting the National Defense of the United States within the meaning of the Espionage Act, USC 50:31 and 32. Its transmission or the revelation of its contents in any manner to an unauthorized person is prohibited by law. Information so classified

may be imparted only to persons in the military and naval Services of the United States, appropriate civilian officers and employees of the Federal Government who have a legitimate interest therein, and to United States citizens of known loyalty and discretion who of necessity must be informed thereof.

~~RESTRICTED~~

RESTRICTED

NATIONAL ADVISORY COMMITTEE FOR AERONAUTICS

TECHNICAL NOTE NO. 968

THE INWARD BULGE TYPE BUCKLING OF MONOCOQUE CYLINDERS

III - REVISED THEORY WHICH CONSIDERS

THE SHEAR STRAIN ENERGY

By N. J. Hoff and Bertram Klein

SUMMARY

In the present third part of an investigation dealing with the inward bulge type buckling of monocoque cylinders the theory of buckling in pure bending is refined through the consideration of the shear strain energy stored in the sheet covering, the assumption of a revised deflected shape of the rings at buckling, and the use of summations in place of some of the integrations of the preceding reports. The calculation of the shear strain energy is based on an estimated variation of the shear rigidity of the buckled panels of sheet with increasing compressive stress, which makes it possible to dispense with the empiricism involved in the procedure of the preceding papers according to which the value of the parameter n had to be determined from data obtained in general instability tests. The revised theory is applied to all the sheet-covered specimens tested in pure bending in the Guggenheim Aeronautics Laboratory of the California Institute of Technology and at the Polytechnic Institute of Brooklyn. The agreement between theory and experiment is found to be good.

INTRODUCTION

In the present part III of a series of investigations dealing with the inward bulge type buckling of monocoque cylinders an attempt is made to develop further the theory of general instability in pure bending. The basic ideas of the theory were first published in 1938 in reference 1. The

RESTRICTED

monocoque was assumed to consist of a circular sheet metal cylinder reinforced with evenly spaced rings and stringers, one of the stringers being located at the bottom (and most highly compressed) fiber of the cylinder. The buckling load was calculated with the aid of the Rayleigh-Ritz-Timoshenko method. In the axial direction the shape of the inward bulge that develops at buckling was assumed to be sinusoidal. In a transverse section the distortions were assumed to follow the general pattern shown in figure 1a. The dotted line in figure 1b presents more accurately, and on an enlarged scale, the deflections of a ring according to the formula suggested in reference 1. This formula satisfies the requirements of inextensional deformations and of symmetry and represents a distorted shape in which the deflection vanishes and the tangent to the deflected shape is perpendicular to the radius of the circular cylinder when $\varphi = \varphi_0$.

In the calculations the shear strain energy stored in the sheet covering was neglected. The buckling load P_{cr} , defined as the force acting upon the most highly compressed stringer at the time when the monocoque buckles, was obtained as a function of two parameters. One of these was denoted n and defined as π/φ_0 . It characterizes the length of the perimeter involved in buckling as shown in figure 1a. The other was the number m of rings involved in the inward bulge. The buckling load was minimized by differentiating it with respect to n and setting the differential coefficient equal to zero. This equation, together with the original expression for the buckling load, permitted the drawing of a family of curves representing the equivalent length factor λ , defined by the equation

$$P_{cr} = \pi^2 EI_{str} / \lambda^2 L_1^2 \quad (1)$$

as a function of the buckling index Λ , defined as

$$\Lambda = (r^4 / L_1^3 d) (EI)_{str} / (EI)_r \quad (2)$$

The parameter of the family of curves was the number m of rings involved in the inward bulge. From the diagram the minimum critical load of any circular monocoque cylinder and the corresponding value of m could be easily determined by selecting the maximum value of λ - that is, the value on the envelope of the family of curves - corresponding to the buckling index Λ of the monocoque cylinder.

Unfortunately a comparison of the theory of reference 1 with the results of the tests carried out in the Guggenheim Aeronautics Laboratory of the California Institute of Technology (see reference 2) showed that the theoretical buckling load amounted only to 11 to 83 percent of the buckling load found in experiment. The reasons for this discrepancy were discussed in reference 3. Simple calculations showed that if the equations for the deflected shape of the rings were assumed to be valid for the sheet covering also, the shear strain energy stored in the sheet greatly exceeded the strain energy stored in stringers and rings. On the other hand, in all the experiments performed hitherto the panels of sheet were in a buckled state in the vicinity of the most highly compressed stringer when general instability occurred. Obviously buckling of a curved panel of sheet reduces its resistance to shearing deformations, particularly if the radius of the cylinder is small and the stringer spacing large. Consequently, a calculation of the shear strain energy cannot correspond to reality if based upon an unchanged value of the shear modulus G and a deflected shape of the sheet represented by the formula suggested for the deflected shape of the rings.

Moreover, the shearing rigidity of the panels varies around the circumference, those close to the most highly compressed stringer offering little, those near the neutral axis of the cylinder a great deal of resistance to shearing deformations. Consequently even in cases when at buckling the shear strain energy stored in the sheet is small as compared to the strain energy stored in stringers and rings, the sheet has a decisive effect upon the length of the perimeter involved in buckling, and thus greatly influences the buckling load of general instability. Because of the great shearing rigidity of the non-buckled panels it is clear that the inward bulge is not likely to extend to the tension side of the monocoque cylinder, but it is not easy to calculate the exact circumferential length of the bulge, or the exact value of n which is tantamount to it. The effect of the sheet upon n was not considered in the theory of reference 1, and this omission resulted in an overestimate of the circumferential length of the bulge and a consequent underestimate of the buckling load.

In reference 3 a revised theory was developed, based on the fundamental assumption that the buckling load can be calculated accurately enough for practical purposes from the strain energy balance in stringers and rings without considering the shear strain energy stored in the sheet covering,

provided the value of the parameter n is known from general instability tests. This theory yielded the following formula for the buckling load:

$$P_{cr} = n^2 \sqrt{\frac{d}{L_1}} \frac{\pi^2 \sqrt{(EI)_{str}(EI)_r}}{r^2} \quad (3)$$

The values of the symbols in this formula representing geometric and mechanical properties of the monocoque cylinder pertaining to each test specimen of the GALOIT test series of reference 2, and the critical load observed in experiment were substituted into equation (3) and the equation was solved for n . The values obtained ranged from 3.12 to 5.59. The variation was attributed to the effect of the parameters d/r and $(t/r)_{c_{max}}$ characterizing the shearing rigidity of the panels, and the values of n were plotted against them in figure 10 of reference 3. The faired-in curves of this figure show an average deviation from the experimental points amounting to 4.4 percent. It was suggested that this figure be used in conjunction with equation (3) for the prediction of the buckling load of monocoque cylinders.

In the present report the development of the theory is carried one step further. The main improvement is the consideration of the shear strain energy stored in the sheet covering permitting the elimination of the empiricism involved in the determination of the value of n from the results of general instability tests. The calculation of the shear strain energy was made possible by the assumption of an expression connecting the effective shear modulus G' of a panel with the normal stress prevailing in the stringers adjacent to the panel. This effective shear modulus multiplied by one-half the square of the average shear strain in the panel, as calculated from the displacements of the four corners of the panel, was taken to represent the shear strain energy stored in the panel. A second improvement was the choice of a new equation for the distorted shape of the rings. (See fig. 1b.) It satisfies the additional requirement that the radius of curvature of the deflected ring be equal to the original radius of the cylinder when $\phi = \phi_0$.

In the development of the theory some of the original integrations were replaced by summations. Consideration was given to the possibility of deviations of the normal stress distribution from the commonly assumed linear law. The results of the theoretical calculations are presented in the

form of tables the use of which permits the evaluation of the minimum critical load for monocoque cylinders having the same number of stringers as the test specimens of the GALCIT and the P.I.B. series. Tables also could be set up easily for cylinders having any other number of stringers. It is considered advisable, however, to delay the presentation of such additional tables until the time when more is known about the variation of the effective shear rigidity of the panels and the actual shape of deflections at the moment when buckling begins, and when more data are available to substantiate the conclusions of the present theory of the inward bulge type general instability.

The present theory was applied to the pure bending test specimens of the GALCIT series and to those of the P.I.B. tests described in reference 4. Good agreement was found between theory and experiment.

This investigation, conducted at the Polytechnic Institute of Brooklyn, was sponsored by and conducted with the financial assistance of the National Advisory Committee for Aeronautics.

SYMBOLS

a_0, a_1	parameters characterizing effective shear rigidity of a panel
A	cross-sectional area of a stringer
b_0, b_1	parameters involved in describing variation of direct strain
c_k	k th coefficient of a Fourier series
d	stringer spacing measured along circumference
E_r	Young's modulus for material of a ring
E_{str}	Young's modulus for material of a stringer
$f(m+1)$	function of number of ring fields involved in failure
$f_r(n)$	function of parameter n arising in connection with ring strain energy

$f_1 sh(s, n)$ } functions of parameters s and n appearing
 $f_2 sh(s, n)$ } in shear strain energy term

$$F_{sh}(s, n) = a_0 f_1 sh(s, n) - a_1 f_2 sh(s, n)$$

$f_{str r}(s, n)$ } functions of parameters s and n appearing
 $f_{str t}(s, n)$ } in stringer strain energy term

$$F_{str}(s, n) = I_{str r} f_{str r}(s, n) + I_{str t} f_{str t}(s, n)$$

$f_w(s, n)$ function of parameters s and n appearing
 in work term

G ordinary shear modulus of a panel

G' effective shear modulus of a panel

h distance of centroid of a stringer from sheet
 covering of cylinder

i index used in summations or products

I_r moment of inertia of ring cross section and
 its effective width of sheet for bending in
 radial direction

$I_{r o}$ moment of inertia of ring cross section without
 its effective width of sheet for bending in
 radial direction

$I_{str o}$ moment of inertia of stringer cross section
 without its effective sheet for bending in
 radial direction

$I_{str r}$ moment of inertia of stringer cross section and
 its effective width for bending in radial
 direction

$I_{str t}$ moment of inertia of stringer cross section and
 its effective width for bending in tangen-
 tial direction

I_{str}	moment of inertia of stringer cross section without its effective width for bending in tangential direction
j	index used in summations or products
k, K, l	integer constants
L	total length of wave in axial direction
L_1	distance between adjacent rings measured axially along cylinder
$(m+1)$	number of ring fields included in length L
M'	function of $(m+1)$ associated with shear strain energy term
n	a parameter characterizing shape of ring deflection which is equal to ratio of total circumference to that involved in buckling, or $n = \pi/\phi_0$
p	a parameter which affects the direct strain or shear rigidity distributions
P_{or}	load carried by most highly compressed stringer and its effective width of sheet at buckling
P'	load carried by any stringer and its effective width of sheet at buckling
r	radius of circular cylinder
R	polar coordinate
s	number of stringer fields included in bulge
S	total number of stringers in structure
t	thickness of sheet covering
u	integer constant
U	strain energy
U_r	strain energy stored in rings

U_{sh}	strain energy stored in sheet covering
U_{str}	strain energy stored in stringers
$V_S =$	$(4/3)\pi r^3$, volume of a sphere of radius r
$2w_0$	ordinary effective width associated with most highly compressed stringer
$2w^1$	modified effective width associated with a stringer
$2\bar{w}^1$	average modified effective width of all stringers
w_r	radial displacement of a point on a ring or a stringer
w_t	tangential displacement of a point on a ring or a stringer
W	virtual work done by external load
x	coordinate measuring distance along axis of cylinder
y	deflection of a straight beam due to bending
16α	maximum deflection of most highly compressed stringer or most highly deflected ring
16β	maximum deflection of any ring
γ	average angle of twist of a panel
δ	shift of neutral axis measured from horizontal geometric axis in terms of radius
ΔL	change in distance between $x = 0$ and $x = L$ due to distortions
ϵ_{max}	strain in most highly compressed stringer at failure
λ	equivalent length factor
Λ	buckling index
ρ	radius of curvature at any point of a ring
φ	angular measure

ϕ_0 angle defining end of circumferential wave
 $d\psi$ change in direction of tangent

DEVELOPMENT OF THE REVISED THEORY

Revised Deflection Pattern of the Rings

The following seven requirements for the distorted shape of the rings were stated in reference 1, though in a slightly different form:

- (1) Distortions must be inextensional. This requirement can be formulated as

$$w_r = - dw_t/d\phi \quad (4a)$$

where w_r and w_t are the radial and the tangential displacements, respectively, of points lying on rings or stringers. The proof of this statement is now given with the aid of figure 2. The part of the elongation of the arc element $ds = r d\phi$ that is due to a radial displacement of the element is

$$[w_r + (1/2)(dw_r/d\phi)d\phi]d\phi$$

The part that is caused by the tangential displacements is

$$w_t + (dw_t/d\phi)d\phi - w_t$$

The requirement that the length of the arc element remain unchanged can, therefore, be expressed as

$$w_r d\phi + (dw_t/d\phi)d\phi = 0 \quad (a)$$

if a term containing the square of $d\phi$ is omitted as a second order small quantity. From this expression equation (4a) follows immediately. The fact that curved bars usually distort inextensionally was first noted by Lord Rayleigh.

- (2) The maximum radial displacement should occur at the location of the most highly compressed stringer:

$$dw_r/d\phi = 0 \quad \text{when } \phi = 0 \quad (4b)$$

- (3) The tangential displacement must vanish at the location of the most highly compressed stringer:

$$w_t = 0 \quad \text{when } \varphi = -0 \quad (4c)$$

- (4) The radial displacement must vanish when $\varphi = \varphi_0$:

$$w_r = 0 \quad \text{when } \varphi = \varphi_0 \quad (4d)$$

- (5) The tangential displacement must vanish when $\varphi = \varphi_0$:

$$w_t = 0 \quad \text{when } \varphi = \varphi_0 \quad (4e)$$

- (6) The tangent to the deflection curve must be perpendicular to the radius of the nondistorted cylinder at the end of the bulge. This requirement may be expressed as

$$dw_r/d\varphi = 0 \quad \text{when } \varphi = \varphi_0 \quad (4f)$$

The proof of this statement is now given with the aid of figure 2. The change in the direction of the infinitesimal arc element is measured by $d\psi$. It follows from the figure that

$$\tan(d\psi) = [(dw_r/d\varphi)d\varphi]/[r + w_r + (dw_t/d\varphi)d\varphi]$$

In the limit the tangent can be replaced by the angle. Because of equation (a) the denominator reduces to r . Consequently

$$d\psi = (1/r)(dw_r/d\varphi) \quad (b)$$

- (7) The radius of curvature of the deflected shape at the end of the bulge must be equal to the original radius of the cylinder.

Since the expression for the curvature ($1/\rho$) is in polar coordinates

$$(1/\rho) = [R^2 + 2(dR/d\varphi)^2 - R(d^2R/d\varphi^2)]/[R^2 + (dR/d\varphi)^2]^{3/2}$$

and since the radial distance R of any point of the distorted median line of the ring from the

origin is the sum of the original radius r and the radial displacement w_r , the curvature can be written as

$$(1/\rho) = (1/r^2)[r - w_r - (d^2 w_r/d\phi^2)] \quad (c)$$

after substitutions are made and powers and products of w_r and its derivatives are omitted as second order small quantities. The requirement for an unchanged curvature is

$$r - w_r - (d^2 w_r/d\phi^2) = 0$$

This requirement is equivalent to the following condition, if requirement (4d) is fulfilled:

$$d^2 w_r/d\phi^2 = 0 \quad \text{when } \phi = \phi_0 \quad (4g)$$

The expression assumed for w_r in the preceding reports satisfied all but the last requirement. Nonfulfillment of equation (4g) is believed to have had little effect upon the buckling load. In the present calculations a new expression for the deflected shape is used which satisfies all the seven conditions. It is found that the shear strain energy corresponding to the new expression is materially smaller than that corresponding to the original expression. The new expression is as follows:

$$w_r = -\beta [2 \cos(n\phi/2) + 9 \cos(3n\phi/2) + 5 \cos(5n\phi/2)] \quad (5)$$

when

$$-(\pi/n) \leq \phi \leq (\pi/n)$$

and

$$w_r = 0 \quad (5a)$$

when

$$|\phi| > (\pi/n)$$

In equation (5)

$$\beta = (\alpha/2)[1 - \cos(2\pi x/L)] \quad (5b)$$

where α is an indeterminate coefficient proportional to the maximum deflection of the cylinder. It may be seen that β represents the same function it represented in reference 1. Consequently the shape of the inward bulge is unchanged

in axial sections of the monocoque cylinder. Because of the requirement given in equation (4a) the tangential displacement w_t can be written as

$$w_t = (\beta/n)[4 \sin(n\varphi/2) + 6 \sin(3n\varphi/2) + 2 \sin(5n\varphi/2)] \quad (6)$$

when

$$-(\pi/n) \leq \varphi \leq (\pi/n)$$

and

$$w_t = 0 \quad (6a)$$

when

$$|\varphi| > (\pi/n)$$

It is easy to prove that equations (5) and (6) satisfy all the conditions presented in equations (4). The old and the new deflected shapes of the rings are compared in figure 1b for the case when $n = 3$.

Obviously the choice of equation (5) is arbitrary. Other different equations can be found which satisfy the seven requirements. It is shown in appendix I how expressions can be determined which, while fulfilling the conditions set forth in equations (4), satisfy additional requirements and correspond to further reduced values of the shear strain energy. These expressions represent deflection curves that hug the original circular shape more closely in the neighborhood of $\varphi = \varphi_0$, as may be seen from the curves given in figure 3.

Strain Energy Stored in the Rings

The strain energy stored in a ring can be calculated from the equation

$$U = \int_0^{\varphi} (1/2)(EI)_r [(1/\rho) - (1/r)]^2 r \, d\varphi \quad (7)$$

where

$(EI)_r$ bending rigidity of ring for bending in the plane of ring

r original radius of cylinder

ρ radius of curvature at any point after distortions

The moment of inertia of the ring is calculated for the ring section proper augmented with its effective sheet. The width of the effective sheet is taken equal to the width of the ring in agreement with the procedure advocated in references 1, 3, and 5. With the aid of equation (c) the strain energy stored in all the rings can be written in the form:

$$U_r = \sum (1/2)(EI)_r \int_{-\pi/n}^{+\pi/n} (1/r^4) [w_r + (\partial^2 w_r / \partial \varphi^2)]^2 r \, d\varphi \quad (8)$$

where the summation must include all the rings involved in 1 wave length. Upon substitution of the value of w_r as given in equation (5), and with the aid of the transformation

$$x = jL/(m+1)$$

valid at the location of any ring, integration gives

$$U_r = (\alpha^2/4)\pi f_r(n) [(EI)_r/2r^3] \sum_{j=1}^m \left\{ 1 - \cos[2\pi j/(m+1)] \right\}^2 \quad (9)$$

where

$$f_r(n) = (1/\pi) \int_{-\pi/n}^{\pi/n} [w_r + (\partial^2 w_r / \partial \varphi^2)]^2 \, d\varphi \quad (9a)$$

In general, if w_r is given by the expression

$$w_r = -\beta \sum_{i=1,2,3,\dots} c_i \cos k_i n \varphi \quad (2k_i \text{ a positive integer}) \quad (A)$$

then equation (9a) becomes

$$f_r(n) = (1/n) \sum_{i=1,2,3,\dots} c_i^2 [(k_i n)^2 - 1]^2 \quad (B)$$

With the values of the coefficients c given in equation (5) equation (B) simplifies to

$$f_r(n) = [1386.875 n^3 - 679 n + (110/n)] \quad (10)$$

The summation indicated in equation (9) was evaluated in the appendix of reference 3. It was found to be equal to

$$(3/2)(m+1) \quad \text{when } (m+1) > 2 \quad (11a)$$

$$1 \quad \text{when } (m+1) = 2 \quad (11b)$$

Thus the total strain energy stored in all the rings within one inward bulge can be written in the following form:

$$U_r = \alpha^2 (3/16) [(m+1)/r^3] (\pi/n) [1386.875 n^4 - 679 n^2 + 110] (\bar{E}I)_r \quad (12)$$

$$\text{when } (m+1) > 2$$

By replacing $(3/2)(m+1)$ by unity in the right-hand member of the equation, the expression for the strain energy valid when $(m+1) = 2$ is obtained.

It is seen that the total strain energy stored in the rings is proportional to the number of ring fields $(m+1)$ involved in one bulge. Moreover, the strain energy increases very rapidly with increasing n ; approximately as the cube of n - that is, it takes very much strain energy to distort the rings into bulges of small circumferential length. For numerical calculations it is convenient to rewrite equation (12) in the form

$$U_r = \alpha^2 (3/16) [(m+1)/r^3] \pi (\bar{E}I)_r f_r(n) \quad \text{when } (m+1) > 2 \quad (13)$$

$$U_r = \alpha^2 [1/(8r^3)] \pi (\bar{E}I)_r f_r(n) \quad \text{when } (m+1) = 2 \quad (13a)$$

where $f_r(n)$ is the function defined in equation (10). Values of this function are tabulated in table 1.

Strain Energy Stored in the Stringers

In accordance with the assumptions made regarding deflections, all the stringers bend both radially and tangentially

(except the most highly compressed stringer which bends, only radially). The strain energy can be calculated from equation (7). It is shown in Strength of Materials that for an originally straight beam

$$(1/\rho) - (1/r) = d^2y/dx^2 \quad (d)$$

if y designates the displacement perpendicular to the x -direction (x being measured parallel to the axis of the beam). As w_r and w_t denote two perpendicular components of the displacements of the stringer, they have to be used in the place of y . Thus the total strain energy stored in the stringers can be written in the form

$$U_{\text{str}} = \sum (1/2) E_{\text{str}} \int_0^L [(\partial^2 w_t / \partial x^2)^2 I_{\text{str } t} + (\partial^2 w_r / \partial x^2)^2 I_{\text{str } r}] dx \quad (14)$$

where the summation must include all the stringers. It is assumed that $I_{\text{str } t}$ and $I_{\text{str } r}$ are principal moments of inertia. After substitution of the expressions given in equations (5) and (6) into equation (14) integration gives

$$U_{\text{str}} = (\alpha^2 \pi^4 / L^3) E_{\text{str}} \sum \left\{ [2 \cos(n\pi/2) + 9 \cos(3n\pi/2) + 5 \cos(5n\pi/2)]^2 I_{\text{str } r} + (1/n^2) [4 \sin(n\pi/2) + 6 \sin(3n\pi/2) + 2 \sin(5n\pi/2)]^2 I_{\text{str } t} \right\} \quad (15)$$

The summation has to be extended around the part of the perimeter involved in buckling. In this region $I_{\text{str } r}$ and $I_{\text{str } t}$ vary since the effective width of sheet added to the cross section of the stringer proper varies because of the changes in the value of the normal stress. The analytical expressions for the moments of inertia are very cumbersome particularly since the effect of the curvature of the sheet covering must also be taken into account. Moreover, the so-called reduced effective width rather than the ordinary effective width must be used for the calculation of the moments of inertia, as was shown in reference 1. Assuming Marguerre's cube-root formula to be valid for the effective width $2w$ of the equivalent flat sheet, the reduced effective width $2w' = (2/3)2w$ in the region where the deflections are in the inward direction. In the region where the cylinder bulges

"out" (see fig. 1a), the "reduced" effective width is $4/3$ of the ordinary effective width and should be denoted properly as "modified" effective width. This term obviously may refer to both the decreased and increased values.

The complexity of the problem can be reduced materially through the assumption of average moments of inertia $I_{str r}$ and $I_{str t}$ corresponding to the average value of the modified effective width. The rule according to which this average must be chosen cannot be determined, however, without carrying out the summations of equation (15) with all mathematical rigor. On the other hand, the critical strain in inward bulge type buckling is not too sensitive to changes in the rule used for determining the average value of the modified effective width, as may be seen from the numerical work of the following chapter, and even less so to changes in the choice of the value of the effective width of the most highly compressed stringer, as was shown in reference 5. Moreover, it should be remembered that the conception of the effective width itself is approximate and in particular the application of the conception to curved panels is lacking in analytical foundation. Consequently great rigor is not called for in the calculation of the effective width.

For these reasons the theory of this report has been developed on the assumption of a constant average value for the moment of inertia. In all the numerical work to follow the average moments of inertia were calculated in correspondence with the estimate that the value of the average modified effective width lies between the values of the ordinary and the reduced effective widths at the location of the most highly compressed stringer. The principles governing the choice of the value within these limits are discussed in connection with details of the numerical work.

The assumption of constant moments of inertia permits a rigorous calculation of the summation indicated in equation (15). The work involved can be slightly simplified through the introduction of the symbols S for the total number of stringers (or stringer fields) in the monocoque cylinder, and s for the total number of stringer fields affected by the distortions. With this notation the angular spacing of the evenly spaced stringers is $2\pi/S$ radians. Moreover, from the definition of n

$$s = S/n \quad (16)$$

With the new notation equation (15) can be rewritten in the form

$$\begin{aligned}
 U_{\text{str}}(L^3/\alpha^2\pi^4)(1/E_{\text{str}}) &= F_{\text{str}}(s,n) = I_{\text{str r}} f_{\text{str r}}(s,n) \\
 &+ I_{\text{str t}} f_{\text{str t}}(s,n) = 256 I_{\text{str r}} + 2 \sum_{i=1}^{(s/2)-1} [2 \cos(\pi i/s) \\
 &+ 9 \cos(3\pi i/s) + 5 \cos(5\pi i/s)]^2 I_{\text{str r}} \\
 &+ (2/n^2) \sum_{i=1}^{(s/2)-1} [4 \sin(\pi i/s) + 6 \sin(3\pi i/s) \\
 &+ 2 \sin(5\pi i/s)]^2 I_{\text{str t}} \quad (17)
 \end{aligned}$$

The term $256 I_{\text{str r}}$ represents the strain energy stored in the most highly compressed stringer. The other terms represent the strain energy stored in all the other stringers. These summations are carried out in appendix II. They give

$$F_{\text{str}}(s,n) = 55 I_{\text{str r}} + 28(s/n^2) I_{\text{str t}} \quad \text{when } s > 4 \quad (18a)$$

$$F_{\text{str}}(s,n) = 400 I_{\text{str r}} + (64/n^2) I_{\text{str t}} \quad \text{when } s = 4 \quad (18b)$$

$$F_{\text{str}}(s,n) = 256 I_{\text{str r}} \quad \text{when } s = 2 \quad (18c)$$

The functions $f_{\text{str r}}(s,n)$ and $f_{\text{str t}}(s,n)$ are tabulated in table 1. With the aid of the function $F_{\text{str}}(s,n)$ defined in equations (17) and (18) the strain energy stored in all the stringers can be given in the concise form

$$U_{\text{str}} = (\alpha^2\pi^4/L^3) E_{\text{str}} F_{\text{str}}(s,n) \quad (19)$$

It is interesting to note that calculation of the strain energy stored in the stringers through integration, based on the assumption of continuously distributed stringers, gives the same expression as that obtained by the preceding summation, provided the number s of stringer fields involved in buckling is equal to or greater than six. It also may be seen that as the ring strain energy was found to be directly proportional to the number of ring fields, so is the stringer strain energy directly proportional to the number of stringer fields involved in distortions (except when the number of stringer fields involved is less than six).

Shear Strain Energy Stored in the Sheet Covering

It was mentioned in the Introduction that the main difference between the approach of the preceding reports and that of the present paper is the consideration in the present paper of the shear strain energy stored in the sheet covering. The calculation of this shear strain energy was made possible through the use of an average value of the shear strain and of an average value of the effective shear modulus for each panel. Figure 4 shows a panel before and after distortions. With the notation of the figure the average angle of shear of the panel may be expressed as

$$\gamma = (1/2L_1) \left\{ \left[(w_t)_{\varphi_1, x_1} + (w_t)_{(\varphi_1 + (2\pi/s), x_1)} \right] - \left[(w_t)_{\varphi_1, x_2} + (w_t)_{(\varphi_1 + (2\pi/s), x_2)} \right] \right\} \quad (20)$$

The total shear strain energy stored in all the panels is

$$U_{sh} = \sum (1/2) \gamma^2 G' L_1 t d \quad (21)$$

where the summation has to be carried out over all the panels involved in the bulge. In this equation G' stands for the effective shear modulus of the panel. When the panel is in the non-buckled state, G' is equal to G . If, however, the compressive stress in the panel exceeds the critical stress, it is reasonable to assume that the panel will offer less resistance to shearing distortions. The decrease in the shear rigidity is likely to depend both on the ratio of

the average compressive stress in the panel to the critical stress of the panel, and on the ratio of the stringer spacing to the radius of curvature of the cylinder. A theoretical evaluation of this dependence appears to be very difficult. An experimental establishment of the connections should be easier, but no publication dealing with the subject is known to the authors. Because of this lack of information it was necessary to assume arbitrarily an expression for the effective shear modulus. It was decided to use the equation

$$G' = G \left[a_0 - a_1 (\cos \varphi) \right]^{1/p} \quad (22)$$

If in this expression a_0 , a_1 , and p are equal to unity, the value of the effective shear modulus is zero at the most highly compressed stringer, and G' at the horizontal diameter of the cylinder. If a_0 is equal to, and a_1 slightly smaller than unity, G' does not become zero even near the most highly compressed stringer. In both cases the variation of G' is linear with vertical distance from the most highly compressed stringer. This linear law can be changed to a parabolic one by assuming p to be greater than unity. Figure 5 shows these possibilities.

It is reasonable to assume that, other things being equal, the value of G' will be small in panels upon which large compressive forces are acting, and large in panels upon which small compressive forces are acting. Thus the linear law for G' just discussed may well represent the case of a cylinder in which the normal stress distribution is linear. The assumption of a parabolic normal strain distribution shown by the dotted line in figure 6 appears to be in reasonably good agreement with the experimental curve shown by the full line in figure 6, if the region alone is considered in which the bulge develops at buckling ($\varphi_0 < 90^\circ$). The curve represents the normal strain distribution in specimen 159 of the GALCIT series and is taken from reference 6. Consequently equation (22) with $p = 2$ might well represent the variation of G' around the circumference of a monocoque cylinder in which the distribution of the normal stress is not linear, and the neutral axis is materially shifted from the center of the cylinder.

In any case, it is hoped that equation (22) can be well enough adapted to experimental curves which might be available in the future. Calculating from equation (22) the

value of the effective shear modulus for the middle of a panel results in

$$G' = G \left\{ a_0 - a_1 \left[\cos \frac{2\pi(i+1/2)}{s} \right]^{1/p} \right\} \quad (22a)$$

Upon substitution of equations (6), (20), and (22a) into equation (21) there results after some simplification

$$U_{sh} = \frac{\alpha^2 G t d}{32 L_1} \sum_{j=0}^m \left(\frac{s}{2} \right)^{-1} \sum_{i=0}^j \frac{2}{n^2} \left\{ 4 \left[\sin \frac{\pi i}{s} + \sin \frac{\pi(i+1)}{s} \right] \right. \\ \left. + 6 \left[\sin \frac{3\pi i}{s} + \sin \frac{3\pi(i+1)}{s} \right] + 2 \left[\sin \frac{5\pi i}{s} + \sin \frac{5\pi(i+1)}{s} \right] \right\}^a \\ \left\{ a_0 - a_1 \left[\cos \frac{2\pi(i+1/2)}{s} \right]^{1/p} \right\} \left[\cos \frac{2\pi(j+1)}{m+1} - \cos \frac{2\pi j}{m+1} \right]^a \quad (23)$$

The summation over the ring fields is carried out in appendix II. With the notation

$$\sum_{j=0}^m \left[\cos \frac{2\pi(j+1)}{m+1} - \cos \frac{2\pi j}{m+1} \right]^a = \frac{f(m+1)}{m+1}$$

the result is

$$\frac{f(m+1)}{m+1} = (m+1) \left(1 - \cos \frac{2\pi}{m+1} \right) \quad \text{when } m+1 > 2 \quad (24a)$$

$$= 8 \quad \text{when } m+1 = 2 \quad (24b)$$

The function $f(m+1)$ approaches $2\pi^2$ when $m+1$ increases without limit. It is graphed in figure 7.

In appendix II the product of the expression in the first of the braces of equation (23) by a_0 was summed up over all the stringer fields. Using the notation $a_{of1sh}(s,n)$

for this sum, write *see appendix p. 43*

$$a_0 f_1 \text{ sh}(s, n) = \left(\frac{2h_0}{n^2} \right) \left\{ 56 + 4[4 \cos(\pi/s) + 9 \cos(3\pi/s) + \cos(5\pi/s)] \right\}$$

provided $s > 4$ (25)

It was not found practicable to sum up the product of the same expression by the second term in the second brace. It was easier to calculate it numerically for the different numbers of stringers contained in the monocoque cylinder and for the different numbers of stringers involved in buckling. The numerical values of these functions are tabulated in table 1. Using the notation $a_1 f_2 \text{ sh}(s, n)$ for the second function, write

$$U_{\text{sh}} = \alpha^2 \frac{G t d}{32 L_1} \frac{f(m+1)}{m+1} \left[a_0 f_1 \text{ sh}(s, n) - a_1 f_2 \text{ sh}(s, n) \right] \quad (26)$$

Equation (26) can be written in a more concise form by using the function $F_{\text{sh}}(s, n)$ defined as

$$F_{\text{sh}}(s, n) = a_0 f_1 \text{ sh}(s, n) - a_1 f_2 \text{ sh}(s, n) \quad (26a)$$

Work Done by the External Forces

The loading of the monocoque cylinder consists of a pure bending moment which is resisted by the stringer plus effective width of sheet combinations. Consequently the work of the external forces is the sum of the products of the normal force acting upon each stringer plus effective width combination by the change in the length of the stringer corresponding to the assumed deflected shape at buckling. In the preceding reports on the inward bulge type of general instability the stringers were assumed to be continuously distributed around the perimeter, and the work was calculated by integration. The accuracy of the theory is now increased by treating the stringers individually, which procedure, of course, necessitates replacing the integration by summation.

The normal force P' acting upon a stringer plus effective sheet combination is assumed to be given by the equation

$$P' = P_{\text{cr}} \left[b_0 + b_1 (\cos \phi) \right] P \quad (27)$$

where P_{cr} is the normal force acting upon the most highly compressed stringer plus effective sheet combination when buckling occurs. The form of equation (27) is similar to that of equation (22). If the normal force is distributed linearly and the symbol δ is used to denote the ratio of the shift of the neutral axis to the radius,

$$b_0 = \delta/(1 + \delta) \quad \text{and} \quad b_1 = 1/(1 + \delta), \quad \text{provided } p = 1.$$

A nonlinear normal force distribution can be represented by the same formula if $p > 1$. Figure 6 serves to illustrate some of these statements. The shortening due to bending of the distance between the end points corresponding to $x = 0$ and $x = L$ of an originally straight bar is given by

$$\Delta L = \int_0^L (dy/dx)^2 dx \quad (e)$$

The effect of displacements in the tangential and in the radial direction is additive. Consequently the work done by the external forces can be written in the form

$$\begin{aligned} W &= \sum P' \Delta L \\ &= (P_{cr}/2) \sum \int_0^L \left[b_0 + b_1 (\cos \varphi)^{1/p} \right] \left[(\partial w_r / \partial x)^2 + (\partial w_t / \partial x)^2 \right] dx \quad (28) \end{aligned}$$

where the summation must include all the stringers involved in buckling. By using equations (5) and (6), the following equation is obtained after integration

$$\begin{aligned} W &= \frac{\alpha^2 \pi^2 P_{cr}}{4L} \left(256(b_0 + b_1) \right. \\ &\quad + 2 \sum_{i=1}^n \left\{ \left[b_0 + b_1 \left(\cos \frac{2\pi i}{s} \right)^{1/p} \right] \left[\left(2 \cos \frac{\pi i}{s} + 9 \cos \frac{3\pi i}{s} + 5 \cos \frac{5\pi i}{s} \right)^2 \right. \right. \\ &\quad \left. \left. + (1/n^2) \left(4 \sin \frac{\pi i}{s} + 6 \sin \frac{3\pi i}{s} + 2 \sin \frac{5\pi i}{s} \right)^2 \right] \right\} \right) \quad (29) \end{aligned}$$

The summation of the terms containing b_0 leads to expressions similar to those given in equations (18). In the case of the terms containing b_1 it is more convenient to carry out the summation numerically for given values of s and S . With the notation

$$f_W(s, n) = 256 + 2 \sum_{i=1}^4 \left\{ \left(\cos \frac{2\pi i}{S} \right)^{1/p} \left[\left(2 \cos \frac{\pi i}{s} + 9 \cos \frac{3\pi i}{s} + 5 \cos \frac{5\pi i}{s} \right)^2 + \left(1/n^2 \right) \left(4 \sin \frac{\pi i}{s} + 6 \sin \frac{3\pi i}{s} + 2 \sin \frac{5\pi i}{s} \right)^2 \right] \right\} \quad (29a)$$

the work done by the external forces may be given in the form

$$W = \frac{\alpha^2 \pi^2 P_{cr}}{4L} \left\{ [55 + (28/n^2)] s b_0 + b_1 f_W(s, n) \right\} \quad (30)$$

when $s > 4$.

When s is equal to or smaller than 4, equation (30) must be modified. The modified forms can be written down without difficulty with the aid of the expressions given in equations (18).

A further simplification of the work expression is possible through a consideration of the effect upon the buckling load of different normal stress distributions. It was shown in reference 4 that deviations from the linear law caused but small changes in the work done by the external forces. Moreover, it follows indirectly from the considerations of reference 5 that the effect upon the external work of a shift of the neutral axis may be similarly neglected. It is reasonable, therefore, to simplify the calculations of the external work through the assumptions of linearity and zero shift - that is, to assume that

$$s = 0 \quad b_0 = 0 \quad b_1 = 1 \quad p = 1 \quad (31)$$

On the other hand, any similar simplifying assumptions in the expression for the reduced shear modulus (equation (22)) lead to considerable changes in the shear strain energy terms. Although it is admitted that there is some connection between equations (22) and (27), it is not considered inconsistent to

keep the general law for the reduced modulus while simplifying the normal stress expression through the assumptions contained in equations (31) because the exact nature of the variation of G' with the normal stress is not known at present.

If, however, equations (31) hold true, equation (30) may be written in the simplified form

$$W = (\alpha^2 \pi^2 / 4L) P_{cr} [f_W(s, n)] \quad (30a)$$

This equation is valid for any positive even value of s ; s cannot assume an odd value because of the symmetry of the buckled shape with respect to the bottom stringer. Numerical values of the function $f_W(s, n)$ are listed in table 1.

Determination of the Buckling Load

The buckling criterion can be written in the form

$$U_{tot} - W_{tot} = 0 \quad (32)$$

By equating the expression of the external work given in equation (30a) to the sum of the right-hand members of equations (13), (19), and (26), the following condition for P_{cr} is obtained:

$$\begin{aligned} & (\alpha^2 \pi^2 / 4L) P_{cr} f_W(s, n) \\ & = \alpha^2 (3\pi/16) (m+1) [(EI)_r / r^3] f_r(n) + (\alpha^2 \pi^4 / L^3) F_{str}(s, n) E \\ & + (\alpha^2 / 32) (Gtd / L_1) \left\{ [f(m+1)] / (m+1) \right\} F_{sh}(s, n) \end{aligned} \quad (33)$$

This equation can be simplified slightly through the assumption that all the elements of the monocoque are made of the same material. Dividing through by $E(A + 2w_c)$, where $2w_c$ is the total (not the reduced or modified) effective width of the most highly compressed stringer, it is possible to solve for the strain ϵ_{cr} in the most highly compressed stringer at buckling. In the divisor the effective width and not the reduced or modified effective width has to be used in accordance with the statements made in reference 1 in connection with this problem.

With $V_S = (4/3)\pi r^3$ the volume of a sphere of radius r , $d = 2\pi r/S$ the perimetric distance between stringers, and $L_1 = L/(m+1)$ the ring spacing, the critical strain ϵ_{cr} becomes after some manipulation

$$\epsilon_{max} = \left\{ (L_1/V_S)f_r(n)(m+1)^2 I_r + (2\pi/L_1)^2 F_{str}(s,n)/(m+1)^2 + 0.0307(tr/S)f(m+1)F_{sh}(s,n) \right\} / [A+2wt]f_w(s,n) \quad (34)$$

According to equation (34) the critical strain ϵ_{cr} is a function of the two parameters $(m+1)$ and s . These parameters must assume integral values that make the critical strain a minimum. The critical strain can be minimized without difficulty with respect to $(m+1)$ if the assumption is made that $(m+1)$ may assume any (integral or non-integral) value. The critical strain then becomes a continuous function of the parameter $(m+1)$ so that the minimum condition can be obtained through differentiation. Hence

$$\begin{aligned} \partial \epsilon_{max} / \partial (m+1) = 0 = & 2(L_1/V_S)(m+1)f_r(n)I_r \\ & - 2(2\pi/L_1)^2 F_{str}(s,n)/(m+1)^3 \\ & + 2(0.0307)(tr/S) \left\{ (m+1) [1 - \cos(2\pi/(m+1))] \right. \\ & \left. - \pi \sin(2\pi/(m+1)) \right\} F_{sh}(s,n) \quad m+1 > 2 \quad (35) \end{aligned}$$

If the symbol M' is introduced by the definition

$$M' = (m+1)^3 \left[(m+1) \left(1 - \cos \frac{2\pi}{m+1} \right) - \pi \sin \frac{2\pi}{m+1} \right] \quad (36)$$

and the value of the function M' is calculated for different values of $(m+1)$, the function will be found almost constant. This may be seen from table 2. Since $M'/(m+1)^3$ appears in equation (35) in a term which is usually small, the accuracy of the calculations is not impaired by replacing M' by the constant value 60. This substitution reduces equation (35) to the simple fourth degree equation

$$(m+1)^4 = \left[(2\pi/L_1)^2 F_{str}(s, n) - 1.8(tr/S)F_{sh}(s, n) \right] / \left[(L_1/V_S) f_r(n) I_r \right] \quad (37)$$

Equation (37) in conjunction with equation (34) would represent the complete solution of the problem of the inward bulge type buckling of a monocoque cylinder if the correct value of the parameter s were known. This value, however, can be determined relatively easily with the aid of the trial-and-error method suggested in the following section.

If greater accuracy is desired, equation (37) can be used as a first approximation for $(m+1)$. Then the correct value of M' can be taken from table 2 and equation (37) written in the modified form

$$(m+1)^4 = \left[(2\pi/L_1)^2 F_{str}(s, n) - (0.0307)M'(tr/S)F_{sh}(s, n) \right] / \left[(L_1/V_S) f_r(n) I_r \right] \quad (37a)$$

This was done in the numerical calculations.

Procedure for Calculating the Critical Strain

As stated previously, the monocoque cylinder discussed in this report is assumed to have a stringer placed at the bottom ($\phi = 0$). The value of s representing the stringer fields involved in buckling must be, therefore, an even integer. On the other hand, deformations at buckling are not likely to extend to the tension side of the monocoque because of the great shearing rigidity of the non-buckled panels. The investigations reported in reference 3 even showed that $\phi_0 = \pi/n$ usually varied only between 35° and 70° . Consequently the number of the values s may assume is restricted sufficiently to permit a trial-and-error procedure based on simple guessing if the number S of stringers contained in the monocoque is not too large. This was the case with all the GALCIT and P.I.B. specimens. One, two, or three likely values were assumed for s , the corresponding values of $(m+1)$ were determined from equation (37), and the critical strain was calculated for each of the assumptions by substituting the values of the proper functions of $(m+1)$ into equation (34). The smallest of the critical strains so obtained was considered the actual critical strain of the monocoque cylinder.

When the monocoque cylinder contains a greater number of stringers, there may be too many possible values for s to permit close guessing. In such cases recourse may be had to the semiempirical data presented in figure 10 of reference 3 and in figure 18 of reference 5. The predicted value of n can be taken from the figure if the geometric and mechanical properties of the structure, and the maximum strain ϵ_{cr} are known. The maximum strain in turn may be calculated approximately from the equation

$$\epsilon_{cr} = \frac{1}{A} n^2 \sqrt{\frac{d}{L_1}} \frac{\pi^2 \sqrt{I_{str} I_{r'o}}}{r^2} \quad (38)$$

where the subscript o signifies that the moments of inertia of stringer and ring are calculated without consideration of the effective width of sheet. With an approximate value for n thus calculated, the minimum critical strain can be determined by comparing values obtained from equations (34) and (37a) upon substitution of integral values of s close to the value $s = S/n$.

To reduce to a minimum the work involved in the application of the procedure, tables 1 and 2 have been prepared, which enable the stress analyst to obtain directly the numerical values of most of the functions needed for a solution of the problem.

COMPARISON WITH EXPERIMENT

Remarks

The present theory was applied to all the sheet-covered specimens tested in pure bending at GALCIT, specimens 26 through 68, the data for which are given in reference 2, and the two types of specimens tested at P.I.B., the data for which can be found in reference 4. The computations are presented in table 3. The following remarks may be of help in understanding details of the numerical work involved in the application of the theory.

The effective width of sheet to be added to the ring section was assumed to be equal to the width of the ring section, as already mentioned. The effective width of sheet to be added to the stringer section was calculated according

to the procedure presented in reference 5. The average reduced (or modified) effective width was assumed to be equal to the reduced effective width at the most highly compressed stringer when the number of stringers involved in the bulge was small. This assumption certainly underestimates the average bending rigidity of the stringers, and consequently leads to a conservative value of the buckling stress. Nevertheless, the deviation from reality should not be too great since the strain energy of bending is small in the stringers far from the most highly stressed stringer. The influence of the stringers upon which less than the maximum compressive force is acting is more noticeable when there are many stringers involved in the bulge. In such cases the average reduced effective width was assumed greater, as a maximum equal to the total (non-reduced) effective width of the most highly compressed stringer.

In the expression for the reduced shear modulus G' the constant a_0 in equation (22) was assumed to be equal to unity. Similarly a_1 was taken as unity whenever S was equal to or smaller than 24. For $S = 40$ the value of a_1 was assumed to be between 0.80 and 1.00. The difference in this choice is based on the difference in the movability of the buckled panels. Obviously much less movability results from the buckling of a narrow panel in a cylinder having 40 stringers than from the buckling of a wide panel in a cylinder having only 10 stringers, provided the radius of the cylinder is the same. The ratio of the maximum stress to the buckling stress of the curved panel also has an effect upon the shearing rigidity and was approximately taken into account in the choice of a_1 in the case of the cylinders having 40 stringers.

As discussed earlier, the assumption of $p = 2$ in equation (22) may represent a curvilinear shear rigidity distribution, possibly corresponding to a nonlinear normal stress distribution in the bent monocoque cylinder, a noticeable shift in the location of the neutral axis, or a combination of the two. Since in the case of test specimens having but 10 stringers the neutral axis must be considerably shifted under the bending moment that causes general instability, p was assumed to be 2 for the 10-stringer monocoques. In the case of test cylinders having 20 stringers the critical strain in general instability was usually calculated on the basis of both assumptions $p = 1$ and $p = 2$.

The calculation of the external work term was based on the assumptions represented by equations (31).

Application of the present theory to specimen 28 indicated that the smallest buckling load would be obtained when only one ring was involved in failure. Hence in this case the strain energy stored in the ring (col. 25) had to be calculated according to equation (11b) instead of equation (11a).

Illustrative Example

For a better understanding of the numerical work presented in table 3 details of the calculations are explained using specimen 31 as an example. Reference 2 gives $S = 20$, $L_1 = 4$ inches, $r = 15.92$ inches, and $t = 0.01$ inch. The ring and stringer sections are those designated as T_5 and S_1 , respectively. The first three columns in table 3 contain data of the specimen. Column 4 gives the value of $(2\pi/L_1)^2 = 2.467$ as taken from table 1A. In the fifth column the assumed value of s must be filled in. As a first trial s is assumed to be 4, which is just about the smallest possible choice. This gives $\phi_0 = (4/20)\pi = 36^\circ$, and, as was stated earlier, from the investigations of reference 3 it follows that ϕ_0 should have a value between 35° and 70° .

The (ordinary) effective width is approximately calculated to be 2 inches. In estimating $2w'$, the average modified effective width, the choice lies between $2w_0 = 2$ inches and $(2w_0)'$, which is approximately 1.5 inches. Because of the prevalence in the strain-energy-in-stringer terms of the most highly compressed stringer against the only one additional stringer involved in buckling on each side of the plane of symmetry, $2w' = 1.7$ inches appears a reasonable suggestion and hence is adopted.

Column 9 contains $I_{str r}$ which is taken from figure 7 of reference 5, or else may be calculated from equation (34) of reference 5:

$$I_{str r} = I_{str r o} + \frac{\left\{ h + (t/2) - \left[\frac{(2w)^2}{(24r)} \right] \right\}^2}{(1/2wt) + (1/A)} + (4/5) \left[\frac{(2w)^2}{(24r)} \right]^2 (2wt)$$

where h is the distance of the centroid of the stringer from the sheet covering of the cylinder. Table 1 gives $f_{str r}(s,n) = 400$ when $S = 20$ and $s = 4$. The product of this value by $I_{str r}$ is filled in, in column 10. In column 11 $I_{str t}$ is listed after calculation from equation (36) of reference 5:

$$I_{str t} = I_{str t o} + (1/12)(2w)^3 t$$

where $I_{str t o}$ is the moment of inertia of the stringer without the effective width of sheet for bending in the tangential direction. Multiplication of this value by $f_{str t}(s,n)$, which is found in table 1 to be 2.56, yields the value appearing in column 12. Column 13 is then the sum of columns 10 and 12.

The values found in columns 15 and 18 are those given in table 1 corresponding to $a_1 = p = 1$. Column 19 is the value in column 15 less that in column 18. If several steps in the calculations are anticipated, $(m+1)$ can be estimated to be about 5 so that from table 2 M^1 is about 58. The product of columns 14 and 19 is listed in column 20, the value of M^1 in column 21. Column 22, the product of columns 20 and 21, contains one of the terms in equation (37a), the equation from which $(m+1)$ will be calculated. Column 23 lists $f_r(n)$ as taken from table 1. The value of I_r in column 24 was calculated according to the suggestions of reference 5 - that is, the effective width of the sheet was assumed to be equal to the width of the stringer. With the value of V_s taken from table 1A the value to be filled in, in column 25 can be easily computed. This is the second term needed for the calculation of $(m+1)$. The third term is obtained by multiplying together the values found in columns 4 and 13, and is listed in column 26. Subtracting the value listed in column 22 from that in column 26, and dividing the difference by the value in column 25, gives $(m+1)^4$. These operations are listed in columns 27 and 28. It should be noted how small the value in column 22 is as compared to that in column 26. Now $(m+1)^2$ and $(m+1)$ are obtained and listed in columns 29 and 30.

In order to calculate ϵ_{max} from equation (34), the values listed in columns 20, 25, and 26 must be multiplied by the proper functions of $(m+1)$. Thus column 31 contains

the value of column 25 multiplied by $(m+1)^2$, column 32 the value of column 26 divided by $(m+1)^2$, and column 34 the value of column 20 multiplied by $f(m+1)$. The value of this latter function is taken from figure 7 and is listed in column 33. The sum of the values in columns 31, 32, and 34 is given in column 35. Column 36 lists $2w_0 = 2$ inches as assumed at the beginning of this numerical example, column 37 the cross-sectional area of the stringer plus effective width combination. This is 0.0524 square inch since the cross-sectional area of the stringer alone is 0.0324 square inch, and the thickness of the sheet is 0.010 inch. Column 38 contains the value of the function $f_w(s, n)$ as taken from table 1. Finally, a multiplication and a division, carried out in columns 39 and 40, yields the value of the theoretical critical strain ϵ_{max} . In the present case $\epsilon_{max} = 0.00245$ is obtained (col. 40).

In column 41 the experimental critical strain is listed. For specimen 31 it is 0.00190, a value definitely smaller than the one obtained theoretically. On the other hand, $s = 4$ may not be the correct choice. Indeed, figure 10 of reference 3 gives $n = 3$, approximately, if the geometric and mechanical properties of specimen 31, and the experimental critical strain are used. The choice of $s = 6$ should be best, therefore, since it yields $n = 20/6 = 3\frac{1}{3}$, which is close to the value 3. In table 3 the entire calculation is repeated now on the assumption that $s = 6$, and not 4, and all the other assumptions are kept unchanged. This time $(m+1)$ becomes 7.1, and the theoretical critical strain $\epsilon_{max} = 0.00217$. This is about 14 percent higher than the experimental strain. The reported number $(m+1)$ of ring fields involved in buckling is 9 as given in column 43.

To make sure that $s = 6$ really gives the minimum critical strain in the inward bulge type instability of this monocoque cylinder, the calculations are once more repeated, this time on the assumption that $s = 8$. This assumption corresponds to $n = 2.5$ and gives $(m+1) = 9.54$ and $\epsilon_{max} = 0.00356$.

CONCLUSIONS

In this report the theory of the inward bulge type of general instability has been extended to include the effects

of the shear strain energy stored in the sheet covering. Tables containing numerical values of the functions involved in the numerical calculations have been prepared which permit an easy and rapid computation of the maximum strain at failure. Comparison of the theory with the experimental results obtained at GALCIT and P.I.B. show an average deviation of 10 percent, and a maximum deviation of 24 percent.

The theory as presented in this report has the following shortcomings:

1. The tables containing the numerical values of the functions involved in the calculations have been prepared only for specimens having the same number of stringers as those of the GALCIT and P.I.B. test series. The tables can be easily expanded to include other numbers of stringers, but it is believed that this work should be undertaken only after the questions listed under (2) and (3) are solved in a satisfactory manner.

2. In the development of the theory an assumption was made concerning the shearing rigidity of a curved panel of sheet which has buckled under the action of shearing stresses. This assumption should be replaced by data to be obtained from experiment.

3. Because of considerations of economy all experimental data available at present on general instability have been obtained with specimens much smaller than actual aircraft structures. The scale effect has necessitated the use of comparatively weak rings and strong stringers. Moreover, all tests have been conducted with cylinders of approximately the same diameter. It is believed that the range of tests must be extended, especially in the direction of larger diameters, before the problem of general instability can be considered as finally solved.

Polytechnic Institute of Brooklyn,
Brooklyn, N. Y., March 1944.

REFERENCES

1. Hoff, N. J.: Instability of Monocoque Structures in Pure Bending. Jour. R.A.S., vol. XLIII, no. 328, April 1938, pp. 291-346.
2. Guggenheim Aeronautical Laboratory, California Institute of Technology: Some Investigations of the General Instability of Stiffened Metal Cylinders.
I - Review of Theory and Bibliography. NACA TN No. 905, 1943.
II - Preliminary Tests of Wire-Braced Specimens and Theoretical Studies. NACA TN No. 906, 1943.
III - Continuation of Tests of Wire-Braced Specimens and Preliminary Tests of Sheet-Covered Specimens. NACA TN No. 907, 1943.
IV - Continuation of Tests of Sheet-Covered Specimens and Studies of the Buckling Phenomena of Unstiffened Circular Cylinders. NACA TN No. 908, 1943.
V - Stiffened Metal Cylinders Subjected to Pure Bending. NACA TN No. 909, 1943.
3. Hoff, N. J.: General Instability of Monocoque Cylinders. (Presented at the Structures Session, Eleventh Annual Meeting of the Institute of the Aeronautical Sciences, Jan. 25 to 29, 1943.) Jour. Aero. Sci., vol. 10, no. 4, April 1943, pp. 105-114, 130.
4. Hoff, N. J., Fuchs, S. J., and Cirillo, Adam J.: The Inward Bulge Type Buckling of Monocoque Cylinders. II - Experimental Investigation of the Buckling in Combined Bending and Compression. NACA TN No. 939, 1944.
5. Hoff, N. J., and Klein, Bertram: The Inward Bulge Type Buckling of Monocoque Cylinders. I - Calculation of the Effect upon the Buckling Stress of a Compressive Force, a Nonlinear Direct Stress Distribution, and a Shear Force. NACA TN No. 938, 1944.
6. Guggenheim Aeronautical Laboratory, California Institute of Technology: Some Investigations of the General Instability of Stiffened Metal Cylinders. VII - Stiffened Metal Cylinders Subjected to Combined Bending and Torsion. NACA TN No. 911, 1943.
7. Hobson, E. W.: A Treatise on Plane Trigonometry. The Univ. Press (Cambridge), 4th ed., 1921.

APPENDIX I

Deflected Pattern of a Ring

It can be shown from the theory of Fourier series that any symmetrically deflected pattern of a circular ring can be represented by:

$$w_r = -\beta \sum_{k=1}^{\infty} C_k \cos(kn\varphi) \quad (A1.1)$$

$$k = 1, 2, 3, \dots, \quad |\varphi| \leq \pi/n$$

From the basic assumption of inextensional deformations (see equation (4a)), it follows that

$$w_t = \beta \sum_{k=1}^{\infty} (C_k/k) \sin(kn\varphi) \quad (A1.2)$$

These functions are seen to satisfy automatically the five conditions, a, b, c, e, and f, laid down in equations (4) of this paper.

Now by imposing the requirement,

$$\left(\frac{d^p w_r}{d\varphi^p} \right) (\varphi = \varphi_0) = 0 \quad (A1.3)$$

where

$$p = 0, 2, 4, 6, \dots, 2(u-1)$$

the remaining two requirements (4d) and (4g) will be fulfilled (provided $u \geq 2$) and at the same time, (u-2) additional conditions will arise.

Let $C_1 = 1$ and $C_k = 0$ if $k > u + 1$. Then this criterion can be written as a set of u linear equations in u unknowns:

$$\begin{aligned}
 & - 1 + C_2 - C_3 + \dots + (-1)^k C_k + \dots + (-1)^{u+1} C_{u+1} = 0 \\
 & - 1 + 2^2 C_2 - 3^2 C_3 + \dots + (-1)^k k^2 C_k + \dots \\
 & \qquad \qquad \qquad + \left[(-1)^{u+1} \right] (u+1)^2 C_{u+1} = 0 \qquad (A1.4)
 \end{aligned}$$

$$\begin{aligned}
 & - 1 + 2^{2(u-1)} C_2 - 3^{2(u-1)} C_3 + \dots + (-1)^k k^{2(u-1)} C_k + \dots \\
 & \qquad \qquad \qquad + \left[(-1)^{u+1} \right] (u+1)^{2(u-1)} C_{u+1} = 0
 \end{aligned}$$

The common determinant of this system is:

$$\Delta = \pm 1 \begin{vmatrix} 2^0 & 3^0 & \dots & (u+1)^0 \\ 2^2 & 3^2 & \dots & (u+1)^2 \\ 2^4 & 3^4 & \dots & (u+1)^4 \\ \vdots & \vdots & \dots & \vdots \\ 2^{2(u-1)} & 3^{2(u-1)} & \dots & (u+1)^{2(u-1)} \end{vmatrix} \qquad (A1.5)$$

If u is even, the plus sign is valid if u/2 is even, the minus if u/2 is odd. If u is odd, the plus sign is valid if (u-1)/2 is even, the minus if (u-1)/2 is odd.

It will now be shown that equation (A1.5) can be written as the double product:

$$\Delta = \pm \prod_{i=2}^u \prod_{j=3}^{(u+1)} (j^2 - i^2), \quad j > i \qquad (A1.6)$$

where the capital pi's signify a double series of multiplications:

$$\prod_{i=2}^u \prod_{j=3}^{(u+1)} = [(3^2 - 2^2)][(4^2 - 2^2)(4^2 - 3^2)][(5^2 - 2^2)(5^2 - 3^2)(5^2 - 4^2)] \dots$$

$$[(u+1)^2 - 2^2][(u+1)^2 - 3^2] \dots [(u+1)^2 - u^2] \qquad (A1.6a)$$

This is equivalent to the combination of the difference of the squares of all the numbers 2, 3, 4, ..., (u+1) taken two at a time.

The (i-1)th column of the determinant consists of the consecutive elements formed by raising the number i to all even powers from 0 to 2(u-1). If this number i is replaced by either of the numbers ±j, then the (i-1)th and (j-1)th columns will become identical. When two columns of a determinant are identical, its value becomes zero.

Now it is obvious that when Δ is expanded out by the method of minors, it will take the form:

$$P[2, 3, \dots, i, \dots, (u+1)] = \Delta$$

where P consists only of powers and products of the numbers 2, 3, ..., i, ..., (u+1). Consider this as a polynomial in i of deg 2(u-1). Then it must contain exactly 2(u-1) roots. But it was seen that i = ±j is a pair of roots of Δ. Hence all the roots must be included in the set of (u-1) numbers the values of which j can take on.

Corresponding to these roots there will be the factors (j-i) and (j+i) or, what is equivalent to this set, the factors (j²-i²), the latter u-1 in number. It is seen that all columns of Δ are similarly constructed in that they have a constant number raised to the same even powers. Thus all the factors of Δ will be of the form given by (A1.6). There still remains the question whether (A1.6) might be multiplied by some constant factor. If the first numbers in each parenthesis of (A1.6) are multiplied together, there results the term

$$T = (2^0)(3^2)(4^4)(5^6)(6^8) \dots (i^{2k}) \dots (u+1)^{2(u-1)}$$

which is the principal diagonal term of Δ, which term is known to be positive. Consequently (A1.6) represents the correct evaluation of Δ. In an analogous manner, the numerator determinant for any coefficient, C_k, can be put in the form:

$$\Delta C_k = \pm \prod_{i=1}^{(u)} \prod_{\substack{j=2 \\ j \neq k}}^{(u+1)} (j^2 - i^2), \quad j > i, \quad \begin{matrix} j \neq k \\ i \neq k \end{matrix} \quad (A1.7)$$

where the sign is the same as that of equation (A1.6). Thus equation (A1.7) divided by equation (A1.6) gives

$$C_k = \frac{(u+1)}{\prod_{i=2}^k (i^2 - 1)} \bigg/ \frac{u+1}{\prod_{i=2}^k |i^2 - k^2|}, \quad i \neq k \quad (\text{A1.8})$$

In the denominator the absolute values were used as indicated by the bars. This is permissible, since C_k must be positive because Δ and ΔC_k have the same sign as stated. The values of the coefficients are now calculated for three cases:

$$\text{For } u = 2, \quad C_2 = 1.6, \quad C_3 = 0.6 \quad (\text{A1.9a})$$

$$\text{For } u = 3, \quad C_2 = 2, \quad C_3 = 9/7, \quad C_4 = 2/7 \quad (\text{A1.9b})$$

$$\text{For } u = 4, \quad C_2 = 16/7, \quad C_3 = 27/14, \quad C_4 = 16/21, \quad C_5 = 5/42 \quad (\text{A1.9c})$$

Thus the equation

$$w_r = -\beta [\cos(n\varphi) + 1.6 \cos(2n\varphi) + 0.6 \cos(3n\varphi)] \quad (\text{A1.10a})$$

satisfies all seven conditions enumerated in equations (4a) to (4f). The function

$$w_r = -\beta [\cos(n\varphi) + (16/7) \cos(2n\varphi) + (27/14) \cos(3n\varphi) + (16/21) \cos(4n\varphi) + (5/42) \cos(5n\varphi)] \quad (\text{A1.10b})$$

will fulfill two additional requirements at $\varphi = \varphi_0$.

Equations (A1.10a) and (A1.10b) are plotted in figure (2). It is seen how closely the latter curve hugs the original cylinder in the region of the termination of the bulge. It is evident that the more conditions are assumed at the end of the bulge, the smoother the curve will become. In the limit, when an infinite number of derivatives are made to vanish at $\varphi = \varphi_0$, the deflected shape probably will become coincident with the original circular ring (except perhaps in an interval close to $\varphi = 0$).

In reality, however, the deformed pattern will be such that only a few of the derivatives vanish at the end point. The correct number of terms to be used should be determined from considerations of the minimum of the total potential of the system. This cannot be done without the knowledge of the law governing the shearing rigidity of the buckled panels.

APPENDIX II

CALCULATION OF SUMMATIONS

Introduction

In order to carry out all subsequent summations, use shall be made of the fundamental identities:

$$\begin{aligned} \cos x + \cos(x + a) + \cos(x + 2a) + \cdots + \cos [x + (n - 1)a] \\ \equiv \cos [x + (n - 1)a/2] \sin(na/2) \csc(a/2) \end{aligned} \quad (A2.1a)$$

$$\begin{aligned} \sin x + \sin(x + a) + \sin(x + 2a) + \cdots + \sin [x + (n - 1)a] \\ \equiv \sin [x + (n - 1)a/2] \sin(na/2) \csc(a/2) \end{aligned} \quad (A2.1b)$$

Proof of these identities may be found in reference 7. If $x = 0$, and $(n - 1)$ is replaced by N , there result the forms:

$$\begin{aligned} \sum_{i=0}^N \cos(ia) &\equiv \cos(Na/2) \sin [(N + 1)a/2] \csc(a/2) \\ &\equiv (1/2) [1 + \cos(Na) + \sin(Na) \cot(a/2)] \end{aligned} \quad (A2.2a)$$

$$\begin{aligned} \sum_{i=0}^N \sin(ia) &\equiv \sin(Na/2) \sin [(N + 1)a/2] \csc(a/2) \\ &\equiv (1/2) [1 - \cos(Na) + \sin(Na) \cot(a/2)] \end{aligned} \quad (A2.2b)$$

Consequently:

$$\sum_{i=0}^{(s/2)-1} \cos(2\pi iK/s) \equiv \cos[(s/2)-1](\pi K/s) \sin(s/2)(\pi K/s) \csc(\pi K/s) \quad (A2.3)$$

$$\left. \begin{aligned} &= 0, \text{ if } K \text{ is even} \\ &= 1, \text{ if } K \text{ is odd} \end{aligned} \right\} \text{ when } K \neq 1s \quad (A2.3a)$$

$$= s/2, \text{ when } K = 1s \quad (A2.3b)$$

$$= s/2, \text{ when } K = 1s \quad (A2.3c)$$

where K , l , and s are positive integers. Subtracting 1 from equation (A2.3),

$$\sum_{i=1}^{(s/2)-1} \cos(2\pi i K/s) = -1, \text{ if } K \text{ is even} \quad (A2.4a)$$

$$= 0, \text{ if } K \text{ is odd} \quad (A2.4b)$$

$$= (s/2)-1, \quad \text{when } K = ls \quad (A2.4c)$$

where $K \neq ls$

Also from (A2.1a):

$$\sum_{i=0}^{(s/2)-1} \cos(2\pi K/s)(i + 1/2) \equiv \cos[(\pi K/s)$$

$$+ (s/2 - 1)(\pi K/s)] \sin(s/2)(\pi K/s) \csc(\pi K/s)$$

$$= 0 \text{ for all } K, K \neq ls \quad (A2.5a)$$

$$= (-1)^l (s/2) \text{ for } K = ls \quad (A2.5b)$$

Terms Involved in the Strain Energy

Stored in the Stringers

With the aid of equations (A2.4a) to (A2.4c) of this appendix, the summations appearing in equation (17) of this report can now be calculated.

$$\begin{aligned}
 & 256 I_{str r} + 2 I_{str r} \sum_{i=1}^{(s/2)-1} [2 \cos(\pi i/s) + 9 \cos(3\pi i/s) + 5 \cos(5\pi i/s)]^2 \\
 & + (2/n^2) I_{str t} \sum_{i=1}^{(s/2)-1} [4 \sin(\pi i/s) + 6 \sin(3\pi i/s) + 2 \sin(5\pi i/s)]^2 \\
 \equiv & 256 I_{str r} + 2 I_{str r} \sum_{i=1}^{(s/2)-1} [2^2 \cos^2(\pi i/s) + 9^2 \cos^2(3\pi i/s) \\
 & + 5^2 \cos^2(5\pi i/s)] \\
 & + 2 I_{str r} \sum 2 [(2)(9) \cos(\pi i/s) \cos(3\pi i/s) \\
 & + (2)(5) \cos(\pi i/s) \cos(5\pi i/s) + (9)(5) \cos(3\pi i/s) \cos(5\pi i/s)] \\
 & + (2/n^2) I_{str t} [4^2 \sin^2(\pi i/s) + 6^2 \sin^2(3\pi i/s) + 2^2 \sin^2(5\pi i/s)] \\
 & + (2/n^2) I_{str t} \sum 2 [(4)(6) \sin(\pi i/s) \sin(3\pi i/s) \\
 & + (4)(2) \sin(\pi i/s) \sin(5\pi i/s) + (6)(2) \sin(3\pi i/s) \sin(5\pi i/s)] \\
 \equiv & I_{str r} \left\{ 256 + 2 \sum (1/2)(2^2 + 9^2 + 5^2) + 2 \sum (1/2) [2^2 \cos(2\pi i/s) \right. \\
 & \left. + 9^2 \cos(6\pi i/s) + 5^2 \cos(10\pi i/s)] \right. \\
 & + 2 \sum [(2)(9)(\cos 4\pi i/s + \cos 2\pi i/s) + (2)(5)(\cos 6\pi i/s + \cos 4\pi i/s) \\
 & \left. + (9)(5)(\cos 8\pi i/s + \cos 2\pi i/s)] \right\} \\
 & + (I_{str t}/n^2) \left\{ 2 \sum (1/2)(4^2 + 6^2 + 2^2) - 2 \sum (1/2) [4^2 \cos(2\pi i/s) \right. \\
 & \left. + 6^2 \cos(6\pi i/s) + 2^2 \cos(10\pi i/s)] \right. \\
 & + 2 \sum [(4)(6)(\cos 2\pi i/s - \cos 4\pi i/s) + (4)(2)(\cos 4\pi i/s - \cos 6\pi i/s) \\
 & \left. + (6)(2)(\cos 2\pi i/s - \cos 8\pi i/s)] \right\}
 \end{aligned}$$

All these summations fall directly under the types of equations (A2.4a) to (A2.4c). By use of these formulas, there is obtained:

$$F_{str}(s,n) = I_{str r} \left\{ ((s/2) - 1)(2^2 + 9^2 + 5^2) - 2[(2)(9) + (2)(5) + (9)(5)] + 256 \right\} \\ + (I_{str t}/n^2) \left\{ ((s/2) - 1)(4^2 + 6^2 + 2^2) + 2[(4)(6) - (4)(2) + (6)(2)] \right\}$$

if $s > 4$. Or

$$F_{str}(s,n) = (55s)I_{str r} + (28s/n^2)I_{str t} \quad \dots \quad f_{str t} = \frac{28A}{n^2} \cdot 474 \\ (A2.6a) \\ = f_{str r}(s,n) I_{str r} + f_{str t}(s,n) I_{str t}$$

It follows from actual calculations (or equation (A2.4c)) that

$$F_{str}(s,n) = 400 I_{str r} + (64/n^2)I_{str t} \quad \text{if } s = 4 \quad (A2.6b)$$

and

$$F_{str}(s,n) = 256 I_{str r} \quad \text{if } s = 2 \quad (A2.6c)$$

Terms Involved in the Shear Strain Energy
Stored in the Sheet

The summation over i appearing in equation (23) has to be evaluated.

$$+ \frac{1}{4} (s) \cos(\frac{8\pi}{s})(1 + 1/2) + \frac{1}{8} (s) \cos(\frac{16\pi}{s})(1 + 1/2) \dots \}$$

$$\begin{aligned}
 & \sum_{i=0}^{(s/a)-1} \left\{ 4 [\sin(\pi i/s) + \sin \pi (i+1)/s] + 6 [\sin(3\pi i/s) + \sin 3\pi(i+1)/s] \right. \\
 & \qquad \qquad \qquad \left. + 2 [\sin(5\pi i/s) + \sin 5\pi(i+1)/s] \right\}^2 \\
 \equiv & \sum 16 \left\{ (1/2) [1 - \cos(2\pi i/s)] + [\cos(\pi/s) - \cos(2\pi/s)(i+1/2)] \right. \\
 & \qquad \qquad \qquad \left. + (1/2) [1 - \cos(2\pi/s)(i+1)] \right\} \\
 + & \sum 36 \left\{ (1/2) [1 - \cos(6\pi i/s)] + [\cos(3\pi/s) - \cos(6\pi/s)(i+1/2)] \right. \\
 & \qquad \qquad \qquad \left. + (1/2) [1 - \cos(6\pi/s)(i+1)] \right\} \\
 + & \sum 4 \left\{ (1/2) [1 - \cos(10\pi i/s)] + [\cos(5\pi/s) - \cos(10\pi/s)(i+1/2)] \right. \\
 & \qquad \qquad \qquad \left. + (1/2) [1 - \cos(10\pi/s)(i+1)] \right\} \\
 + & \sum (4)(6) \left\{ [\cos(2\pi i/s) - \cos(4\pi i/s)] + [\cos 2\pi(i-1/2)/s \right. \\
 & \qquad \qquad \qquad - \cos(4\pi/s)(i+1/4)] + [\cos(2\pi/s)(i+3/2) - \cos(4\pi/s)(i+3/4)] \\
 & \qquad \qquad \qquad \left. + [\cos(2\pi/s)(i+1) - \cos(4\pi/s)(i+1)] \right\} \\
 + & \sum (4)(2) \left\{ [\cos(4\pi i/s) - \cos(6\pi i/s)] + [\cos(4\pi/s)(i+5/4) \right. \\
 & \qquad \qquad \qquad - \cos(6\pi/s)(i+5/6)] + [\cos(4\pi/s)(i-1/4) - \cos(6\pi/s)(i+1/6)] \\
 & \qquad \qquad \qquad \left. + [\cos(4\pi/s)(i+1) - \cos(6\pi/s)(i+1)] \right\} \\
 + & \sum (6)(2) \left\{ [\cos(2\pi i/s) - \cos(8\pi i/s)] + [\cos(2\pi/s)(i+5/2) \right. \\
 & \qquad \qquad \qquad - \cos(8\pi/s)(i+5/8)] + [\cos(2\pi/s)(i-3/2) - \cos(6\pi/s)(i+3/8)] \\
 & \qquad \qquad \qquad \left. + [\cos(2\pi/s)(i+1) - \cos(8\pi/s)(i+1)] \right\} \\
 \equiv & \sum \left\{ (16 + 36 + 4) + [16 \cos(\pi/s) + 36 \cos(3\pi/s) + 4 \cos(5\pi/s)] \right. \\
 & + [f_1(s) \cos(2\pi/s)(i+1/2) + f_2(s) \cos(4\pi/s)(i+1/2) + f_3(s) \cos(6\pi/s)(i+1/2) \\
 & \left. + f_4(s) \cos(8\pi/s)(i+1/2) + f_5(s) \cos(10\pi/s)(i+1/2)] \right\}
 \end{aligned}$$

where the f 's are functions of s alone.

From equation (A2.5a) it follows immediately that this summation reduces to

$$\left(\frac{s}{2}\right) [56 + 4 (4 \cos \pi/s + 9 \cos 3\pi/s + \cos 5\pi/s)] \quad s > 4 \quad (\text{A2.7a})$$

$$\therefore a_0 f_{1sh}(s,n) = \left(\frac{s}{n^2}\right) [56 + 4 (4 \cos \pi/s + 9 \cos 3\pi/s + \cos 5\pi/s)] \quad s > 4 \quad (\text{A2.7b})$$

Carrying out the summation numerically, it is found that

$$a_0 f_{1sh}(s,n) = a_0 (128/n^2) \quad \text{if } s = 4 \quad (\text{A2.7c})$$

$$= 0 \quad \text{if } s = 2 \quad (\text{A2.7d})$$

There is left the evaluation of the last bracket in equations (23).

$$\begin{aligned} & \sum_{j=0}^{(m+1)-1} [\cos 2\pi(j+1)/(m+1) - \cos(2\pi/(m+1))j]^2 \\ \equiv & \sum_{j=0}^{(m+1)-1} \left\{ (1/2) [1 - \cos 4\pi(j+1)/(m+1)] + (1/2) [1 - \cos 4\pi j/(m+1)] \right. \\ & \left. - \cos(4\pi/(m+1))(j+1/2) - \cos(2\pi/(m+1)) \right\} \end{aligned}$$

$$\equiv (m+1) [1 - \cos(2\pi/(m+1))] - \cos 4\pi/(m+1)$$

$$\sum_{j=0}^{(m+1)-1} [\cos(4\pi/(m+1)) [j + (1/2)]]$$

From equation (A2.5a) it follows that the last bracket vanishes when $(m+1) > 2$. Hence the summation reduces to:

$$f(m+1)/(m+1) = (m+1) [1 - \cos 2\pi/(m+1)] \quad \text{for } (m+1) > 2 \quad (\text{A2.8a})$$

$$f(m+1)/(m+1) = 16 \quad \text{for } (m+1) = 2 \quad (\text{A2.8b})$$

Table 1. Strain Energy Expressions

S	n	STRINGER		SHEAR			RING	WORK
		$f_{str.r}(s,n)$	$f_{str.t}(s,n)$	$f_{1sh}(s,n)$	$f_{2sh}(s,n)$ p = 1	$f_{2sh}(s,n)$ p = 2	$f_r(n)$	$f_w(s,n)$
$s = 4$								
10	2.5	400	10.24	20.480	15.758	17.837	20016.4	380.783
12	3	400	7 1/9	14.222	11.897	12.969	35445.3	386.866
16	4	400	4	8.000	7.249	7.609	86071.5	392.734
20	5	400	2.56	5.120	4.809	4.961	169986.4	395.387
$s = 6$								
10	5/3	330	60.48	143.4	104.209	120.453	5355.1	333.467
12	2	330	42	99.590	80.229	88.993	9434	333.765
16	8/3	330	23.625	56.020	49.745	52.728	24529.8	332.915
20	10/3	330	15.12	35.852	33.255	34.513	49135.4	332.088
24	4	330	10.5	24.898	23.637	24.254	86071.5	331.539
$s = 8$								
16	2	440	56	166.055	138.426	151.153	9434	433.576
20	2.5	440	35.84	106.275	93.259	100.248	20016.4	436.819
24	3	440	24 8/9	73.802	68.204	70.913	35445.3	438.151
40	5	440	8.96	26.569	25.834	26.197	169986.4	439.527

Table I. Strain Energy Expressions (Cont.)

S	n	STRINGER		SHEAR			RING	WORK
		f _{str.r} (s,n)	f _{str.t} (s,n)	f _{1sh} (s,n)	f _{2sh} (s,n) p = 1	f _{2sh} (s,n) p = 2	f _r (n)	f _w (s,n)
s = 10								
20	2	550	70	230.943	195.003	211.672	9434	541.860
24	2.4	550	48.61	160.377	71.409 ?	75.587 ?	17588.4	545.425
40	4	550	17.5	57.736	55.415	56.588	86071.5	548.937
s = 12								
40	10/3	660	30.24	105.778	99.893	102.765	49135.4	657.898
s = 14								
40	20/7	770	48.02	174.0388	161.211	167.426	30445.4	762.753
s = 16								
40	2.5	880	71.68	265.85	240.77	252.77	20016.4	847.524 ?

Table Ia. Auxiliary Expressions

L ₁	1	2	3	4	5	6	7	8	16
(2π/L ₁) ²	39.478	9.869	4.386	2.467	1.579	1.097	0.8057	0.6169	0.1542

r	10	15.92	16
(4/3)πr ³	4188.8	16901	17157

Table 2.

$$M^i = (m+1)^3 \left[(m+1) \left(1 - \cos \frac{2\pi}{m+1} \right) - \pi \sin \frac{2\pi}{m+1} \right]$$

m + 1	3	4	5	6	7	8	9	10	∞
M ⁱ	48.0	54.9	58.4	60.3	61.6	62.3	62.9	63.2	64.9

Table 3. Calculation of the Critical Compressive Strains

[1] GALGIT Spec. No.	[2] S	[3] L ₁ (in.)	[4] (2π/L ₁) ² (in. ⁻²)	[5] s	[6] 2wt (in.)	[7] r (in.)	[8] t (in.)	[9] Istr.r (in ⁴ x10 ⁻⁶)	[10] (9) x f _{str.r} (s,n)
25	40	8	0.6169	10	1.5	15.92	0.01	632	.348
26	40	4	2.467	10	1.5	15.92	0.01	632	.348
27	40	2	9.870	12	1.5	15.92	0.01	632	.417
28	40	16	0.1542	8	2.0	15.92	0.01	669	.294
30	20	8	0.6169	6	2.0	15.92	0.01	669	.278
31	20	4	2.467	4	1.7	15.92	0.01	649	.260
31	20	4	2.467	6	1.7	15.92	0.01	649	.214
31	20	4	2.467	8	1.7	15.92	0.01	649	.286
32	20	2	9.870	6	1.7	15.92	0.01	649	.214
35	10	8	0.6169	4	2.2	15.92	0.01	680	.272
36	10	4	2.467	4	2.2	15.92	0.01	680	.272
37	10	2	9.870	4	2.2	15.92	0.01	680	.272
38	20	1	39.48	6	1.7	15.92	0.01	649	.214
38	20	1	39.48	6	1.7	15.92	0.01	649	.214
39	40	1	39.48	12	0.8	15.92	0.01	546	.361
39	40	1	39.48	12	0.8	15.92	0.01	546	.361
41	40	8	0.6169	10	1.5	15.92	0.015	720	.396
42	40	4	2.467	10	1.5	15.92	0.015	720	.396
43	40	2	9.870	12	1.5	15.92	0.015	720	.475
45	20	8	0.6169	6	2	15.92	0.015	760	.251
45	20	8	0.6169	6	2	15.92	0.015	760	.251
46	20	4	2.467	6	2	15.92	0.015	760	.251
46	20	4	2.467	6	2	15.92	0.015	760	.251
47	20	2	9.870	6	2	15.92	0.015	760	.251
47	20	2	9.870	6	2	15.92	0.015	760	.251
49	10	8	0.6169	4	2.5	15.92	0.015	773	.309
50	10	4	2.467	4	2.5	15.92	0.015	773	.309
51	10	2	9.870	4	2.5	15.92	0.015	773	.309
51	10	2	9.870	4	2.5	15.92	0.015	773	.309
54	40	4	2.467	14	1	16.0	0.010	575	.443
55	40	2	9.870	16	1	16.0	0.010	575	.506
58	20	4	2.467	8	1.5	16.0	0.010	632	.278
59	20	2	9.870	8	1.5	16.0	0.010	632	.278
59	20	2	9.870	8	1.5	16.0	0.010	632	.278
61	20	4	2.467	8	1.5	16.0	0.010	632	.278
61	20	4	2.467	8	1.5	16.0	0.010	632	.278
63	40	4	2.467	14	1	16.0	0.010	575	.443
64	40	2	9.870	16	1	16.0	0.010	575	.506
65	24	4	2.467	8	1	10	0.010	572	.252
66	24	2	9.870	8	1	10	0.010	572	.252
67	12	4	2.467	4	1.7	10	0.010	635	.254
68	12	2	9.870	4	1.5	10	0.010	622	.249
Poly. Specs.									
Thick Sheet	16	5	1.579	6	1.5	10	0.020	2520	.831
Thin Sheet	16	5	1.579	6	1.5	10	0.0120	2190	.723

.22070

47
 .000723
 .000723
 2.5163

Table 3. Calculation of the Critical Compressive Strains

[1] GALCIT Spec.No.	[11] Istr.t (in $\times 10^{-6}$)	[12] (11) $\times f_{str.t}(s,n)$	[13] $F_{str}(s,n) =$ (10)+(12)	[14] $.0307tr/s$ (in $\times 10^{-6}$)	[15] fl.sh(s,n)	[16] a_1	[17] P
25	337	.0590	0.407	122	57.74	0.90	1
26	337	.0590	0.407	122	57.74	0.90	1
27	337	0.102	0.519	122	105.80	0.95	1
28	723	0.065	0.359	122	26.57	0.80	1
30	723	0.0508	0.329	244	35.85	1	1
31	408	.01093	0.277	244	5.12	1	1
31	408	0.0616	0.276	244	35.85	1	1
31	408	0.1465	0.432	244	106.28	1	1
32	408	0.0616	0.276	244	35.85	1	1
35	942	.0965	.369	489	20.48	1	2
36	942	.0965	.369	489	20.48	1	2
37	942	.0965	.369	489	20.48	1	2
38	408	.0616	0.276	244	35.85	1	1
38	408	.0616	0.276	244	35.85	1	2
39	99	.0300	0.391	122	105.78	0.95	1
39	99	.0300	0.391	122	105.78	0.95	1
41	478	.0836	0.480	183	57.74	0.875	1
42	478	.0836	0.480	183	57.74	0.90	1
43	478	.144	0.619	183	57.74	0.90	1
45	1117	.168	0.419	366	35.85	1	1
45	1117	.168	0.419	366	35.85	1	2
46	1117	.168	0.419	366	35.85	1	1
46	1117	.168	0.419	366	35.85	1	2
47	1117	.168	0.419	366	35.85	1	1
47	1117	.168	0.419	366	35.85	1	2
49	2010	.206	0.515	733	20.48	1	2
50	2010	.206	0.515	733	20.48	1	2
51	2010	.206	0.515	733	20.48	1	1
51	2010	.206	0.515	733	20.48	1	2
54	140	.0673	0.510	123	174	1	1
55	140	.100	0.606	123	265.9	1	1
58	337	0.121	0.399	246	106.3	1	1
58	337	0.121	0.399	246	106.3	1	2
59	337	0.121	0.399	246	106.3	1	1
59	337	0.121	0.399	246	106.3	1	2
61	337	0.121	0.399	246	106.3	1	1
61	337	0.121	0.399	246	106.3	1	2
63	140	.0673	0.510	123	174.0	1	1
64	140	.100	0.606	123	265.9	1	1
65	140	.0348	0.287	128	73.80	1	1
66	140	.0348	0.287	128	73.80	1	1
67	408	.0290	0.283	256	14.22	1	1
68	337	.0241	0.273	256	14.22	1	1
Poly. Specs.							
Thick Sheet	728	.172	1.00	384	56.02	1	1
Thin Sheet	509	.120	.843	384	56.02	1	1

Table 3. Calculation of the Critical Compressive Strains

[1] GALCIT Spec.No.	[18] $a_1 f_2 \cdot sh(s,n)$	[19] (15)-(18)	[20] (19)x(14) (in. ² x10 ⁻⁵)	[21] M'	[22] (20)x(21) (in. ²)	[23] $f_r(n)$	[24] I_r (in. ⁴ x10 ⁻⁷)
25	49.87	7.87	96.1	54	.0519	86072	219
26	49.87	7.87	96.1	62	.0596	86072	219
27	94.90	10.88	133	65	.0880	49135	219
28	20.66	5.91	72.2	—	—	169986	219
30	33.26	2.59	63.2	55	.0348	49135	219
31	4.81	0.31	7.5	58	.00435	169986	219
31	33.26	2.59	63.2	62	.0392	49135	219
31	93.26	13.02	318	65	0.207	20016	219
32	33.26	2.59	63.2	65	.0418	49135	219
35	17.84	2.64	129	58	.075	20016	219
36	17.84	2.64	129	65	.084	20016	219
37	17.84	2.64	129	65	.085	20016	219
38	33.26	2.59	63.2	65	.0416	49135	219
38	34.51	1.34	32.7	65	.0216	49135	219
39	95.0	10.78	132	65	.087	49135	219
39	95.0	10.78	132	65	.087	49135	219
41	48.4	9.34	171	53	.091	86071	264
42	49.8	7.94	145	62	.090	86071	264
43	49.8	7.94	145	65	.096	86071	264
45	33.26	2.59	94.6	58	.055	49135	264
45	34.51	1.34	49.0	58	.028	49135	264
46	33.26	2.59	94.6	62	.058	49135	264
46	34.51	1.34	49.0	62	.030	49135	264
47	33.26	2.59	94.6	65	.062	49135	264
47	34.51	1.34	49.0	65	.032	49135	264
49	17.84	2.64	194	58	0.113	20016	264
50	17.84	2.64	194	65	0.128	20016	264
51	15.76	4.72	346	65	0.228	20016	264
51	17.84	2.64	194	65	0.128	20016	264
54	161.2	12.8	158	54	.085	30445	4010
55	240.8	25.1	308	64	.197	20016	4010
58	93.3	13.0	320	58	.186	20016	4010
58	100.2	6.1	150	58	.087	20016	4010
59	93.3	13.0	320	63	.202	20016	4010
59	100.2	6.1	150	63	.095	20016	4010
61	93.3	13.0	320	55	.176	20016	3210
61	100.2	6.1	150	55	.083	20016	3210
63	161.2	12.8	158	55	.087	30445	3210
64	240.8	25.1	308	64	.197	20016	3210
65	68.20	5.6	71.7	59	.042	35445	219
66	68.20	5.6	71.7	65	.047	35445	219
67	11.90	2.32	59.4	59	.035	35445	219
68	11.90	2.32	59.4	65	.039	35445	219
Poly. Specs.							
Thick Sheet	49.75	6.27	240	55	0.132	24530	954
Thin Sheet	49.75	6.27	240	58	0.140	24530	802

Table 3. Calculation of the Critical Compressive Strains

[1] CALCIT Spec.No.	[25] Llfr(n)Ir/vs (in. ² x10 ⁻⁶)	[26] (4)x(13) (in. ²)	[27] (26)-(22)	[28] (27)/(25) =(m+1) ⁴	[29] √(28) =(m+1) ²	[30] √ 29 =(m+1)	[31] (25)x(29) (in. ²)
25	892	.252	.200	224	15.0	3.88	.0134
26	447	1.005	0.945	2120	46.0	6.78	.0206
27	128	5.13	5.04	39400	199	14.1	.0253
28	2350*	.0554	—	—	4	2*	.0047*
30	510	0.203	0.168	329	18.1	4.14	.00923
31	884	.683	.679	769	27.8	5.28	.0246
31	255	.681	.642	2520	50.2	7.10	.0128
31	104	1.066	.859	8250	90.0	9.54	.00944
32	127	2.73	2.69	21200	146	12.1	.0186
35	208	.229	.154	740	27.2	5.22	.00566
36	208	.910	.826	7930	89.1	9.45	.00927
37	51.9	3.64	3.55	68400	262	16.2	.0136
38	63.6	10.9	10.9	171000	414	20.3	.0263
38	63.6	10.9	10.9	171000	414	20.3	.0263
39	63.6	15.4	15.3	24000	490	22.2	.0312
39	63.6	15.4	15.3	24000	490	22.2	.0312
41	1075	.295	.204	190	13.8	3.72	.0148
42	537	1.18	1.09	2030	45.0	6.71	.0442
43	269	6.10	6.00	22300	149	12.2	.0400
45	615	.258	.203	330	18.5	4.30	.0114
45	615	.258	.230	374	19.3	4.40	.0119
46	308	1.03	0.97	3150	56.1	7.48	.0178
46	308	1.03	1.00	3250	57.0	7.55	.0182
47	154	4.14	4.08	26500	163	12.8	.0251
47	154	4.14	4.13	26800	164	12.8	.0253
49	250	0.318	0.205	819	28.6	5.35	.0071
50	125	1.27	1.14	9100	95.5	9.78	.0120
51	62.5	5.09	4.86	77800	279	16.7	.0175
51	62.5	5.09	4.96	79300	282	16.8	.0177
54	2850	1.26	1.17	410	20.3	4.50	.0578
55	935	5.98	5.78	6190	78.6	8.86	.0735 ? see
58	1870	.985	.799	426	20.6	4.55	.0385
58	1870	.985	.898	480	22.0	4.70	.0410
59	935	3.94	3.74	4000	63.3	7.96	.0592
59	935	3.94	3.84	4110	64.0	8.00	.0598
61	1500	.985	.809	539	23.2	4.81	.0348
61	1500	.985	.902	601	24.5	4.95	.0367
63	2280	1.26	1.17	513	22.6	4.75	.0515
64	749	5.98	5.78	7730	87.8	9.36	.0656
65	743	.709	.667	900	30.0	5.48	.0223
66	371	2.83	2.78	7490	86.6	9.30	.0321
67	743	.698	0.663	893	29.9	5.46	.0222
68	371	2.70	2.66	7180	84.6	9.19	.0314
Poly.Specs.							
Thick Sheet	2800	1.58	1.45	517	22.7	4.76	.0635
Thin Sheet	2360	1.33	1.19	504	22.5	4.75	.0530

*See remarks on calculations.

Table 3. Calculation of the Critical Compressive Strains

[1] GALCIT Spec.No.	[32] (26)/(29) (in. ²)	[33] f(m+1)	[34] (33)x(20) (in. ²)	[35] (31)+(32)+(34) (in. ²)	[36] 2w _c (in.)	[37] A _c 2 _{crit} (in. ²)
25	.0168	15.7	.0151	.0453	1.76	.0500
26	.0219	18.3	.0176	.0601	1.76	.0500
27	.0258	19.5	.0259	.0770	1.76	.0500
28	.0138	16	.0116	.0301	2.3	.0554
30	.0112	16.0	.0101	.0305	2.3	.0554
31	.0246	17.4	.00131	.0505	2.0	.0524
31	.0136	18.4	.0116	.0380	2.0	.0524
31	.01172	19.1	.0608	.0819	2.0	.0524
32	.0187	19.4	.0123	.0496	2.0	.0524
35	.0084	17.3	.0224	.0365	3.3	.0654
36	.01022	19.0	.0245	.0440	3.3	.0654
37	.0140	19.6	.0252	.0528	3.3	.0654
38	.0264	19.6	.0124	.0651	2.0	.0524
38	.0264	19.6	.0064	.0591	2.0	.0524
39	.0314	19.6	.0258	.0884	1.0	.0424
39	.0314	19.6	.0258	.0884	1.0	.0424
41	.0214	15.3	.0262	.0624	1.76	.0588
42	.0262	18.2	.0264	.0768	1.76	.0588
43	.0410	19.4	.0282	0.1092	1.76	.0588
45	.0140	16.2	.0153	.0407	2.3	.0670
45	.0134	16.3	.0080	.0333	2.3	.0670
46	.0182	18.6	.0176	.0536	2.3	.0670
46	.0180	18.6	.0091	.0453	2.3	.0670
47	.0254	19.4	.0183	.0688	2.3	.0670
47	.0252	19.4	.0095	.0600	2.3	.0670
49	.0111	17.5	.0340	.0522	3.75	.0886
50	.0133	19.1	.0370	.0623	3.75	.0886
51	.0182	19.6	.0677	.1034	3.75	.0886
51	.0180	19.6	.0380	.0737	3.75	.0886
54	.0620	16.7	.0264	0.1462	1.2	.0444
55	.0761	18.9	.0582	0.2078	1.2	.0444
58	.0478	16.7	.0535	0.1398	2.0	.0524
58	.0446	16.8	.0250	0.1106	2.0	.0524
59	.0623	18.7	.0599	0.1814	2.0	.0524
59	.0615	18.7	.0281	0.1494	2.0	.0524
61	.0425	17.0	.0544	0.1317	2.0	.0524
61	.0403	17.0	.0255	0.1025	2.0	.0524
63	.0558	17.0	.0279	0.1352	1.2	.0444
64	.0681	19.0	.0585	0.1922	1.2	.0444
65	.0236	17.6	.0126	.0585	1.2	.0444
66	.0327	19.0	.0136	.0784	1.2	.0444
67	.0233	17.6	.0105	.0560	2.0	.0524
68	.0314	19.0	.0113	.0746	1.76	.0500
Poly. Specs.						
Thick Sheet	.0694	16.9	.0405	0.1734	2.0	0.181
Thin Sheet	.0590	16.9	.0405	0.1525	2.0	0.165

35

Table 3. Calculation of the Critical Compressive Strains

[1] GALCIT Spec.No.	[38] $f_w(s,n)$	[39] (37)x(38) (in. ²)	[40] $\epsilon_{max} ?$ (37)/(39)	[41] $\epsilon_{exp.}$	[42] (40)/(41)	[43] (m+1) _{exp.}
25	548.9	27.4	.00165	.00170	0.97	6
26	548.9	27.4	.00219	.00208	1.05	8
27	548.9	27.4	.00281	.00288	0.98	
28	439.5	24.4	.00124	.00130	0.95	3
30	332.1	18.4	.00166	.00140	1.18	5
31	395.4	20.7	.00245	.00190		9
31	332.1	17.5	.00217	.00190	1.14	9
31	436.8	22.9	.00356	.00190		9
32	332.1	17.5	.00284	.00256	1.11	16
35	380.8	24.9	.00147	.00120	1.22	6
36	380.8	24.9	.00177	.00164	1.08	7
37	380.8	24.9	.00212	.00200	1.06	17
38	332.1	17.5	.00372	.00283	1.31	
38	332.1	17.5	.00338	.00283	1.19	
39	657.9	27.9	.00315	.00326	0.97	
39	657.9	27.9	.00315	.00326	0.97	
41	548.9	32.3	.00193	.00182	1.06	8
42	548.9	32.3	.00238	.00215	1.11	12
43	657.9	38.6	.00282	.00280	1.01	17
45	332.1	22.3	.00183	.00146	1.25	8
45	332.1	22.3	.00145	.00146	1.00	
46	332.1	22.3	.00240	.00167	1.43	12
46	332.1	22.3	.00203	.00167	1.21	12
47	332.1	22.3	.00308	.00249	1.24	17
47	332.1	22.3	.00270	.00249	1.08	17
49	380.8	33.8	.00154	.00128	1.20	8
50	380.8	33.8	.00184	.00150	1.22	12
51	380.8	33.8	.00306	.00250	1.22	16
51	380.8	33.8	.00218	.00250	0.83	16
54	762.8	33.9	.00430	.003732	1.15	13
55	847.5	37.6	.00551	.004775	1.15	
58	436.8	22.9	.00609	.00435	1.40	11
58	436.8	22.9	.00481	.00435	1.10	11
59	436.8	22.9	.00791	.006154	1.29	16
59	436.8	22.9	.00651	.006154	1.06	16
61	436.8	22.9	.00574	.004927	1.16	7
61	436.8	22.9	.00448	.004927	0.91	7
63	762.8	33.8	.00400	.004045	0.99	9
64	847.5	37.6	.00510	.00510	1.00	14
65	438.2	19.4	.00301	.00315	0.96	
66	438.2	19.4	.00404	.00420	0.96	
67	386.9	20.3	.00276	.00295	0.94	
68	386.9	19.3	.00387	.00375	1.03	
Poly.Specs.						
Thick Sheet	332.9	58.5	.00295	.002568	1.15	4
Thin Sheet	332.9	55.0	.00277	.00224	1.24	4

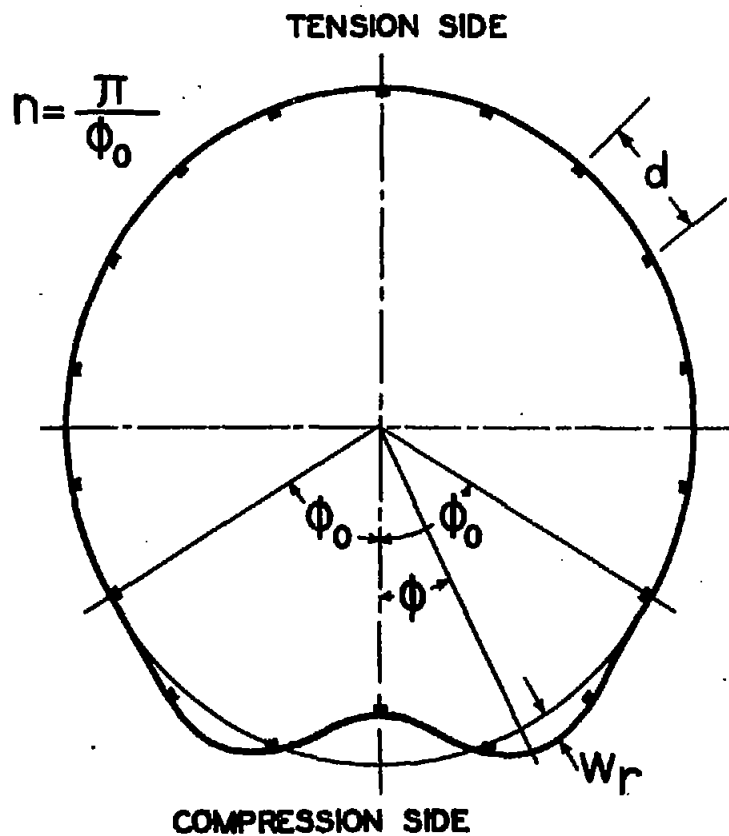


FIG. 1a. DISTORTIONS OF A RING AT BUCKLING.

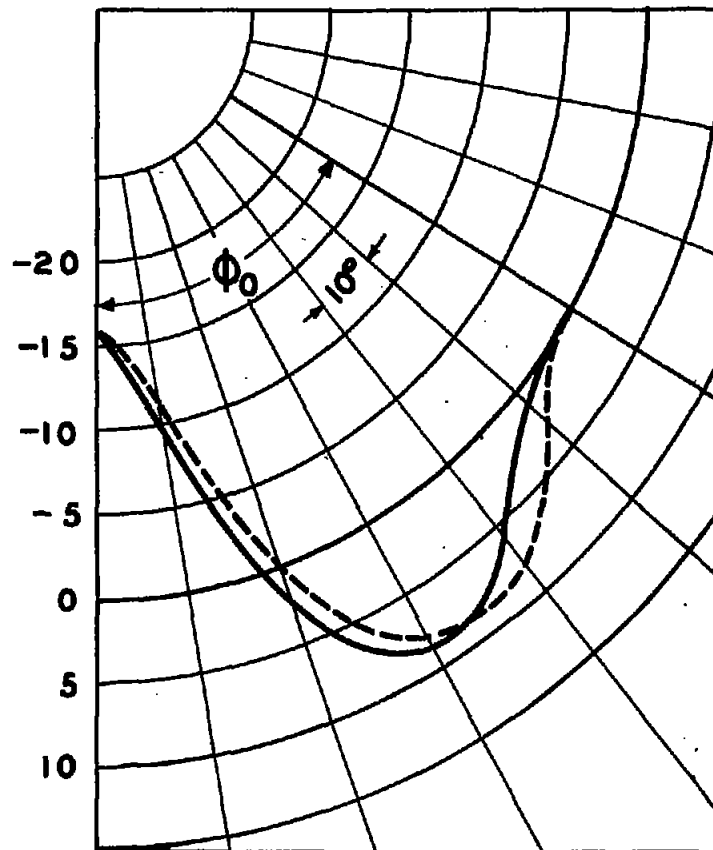


FIG. 1b. COMPARISON OF DEFLECTED PATTERNS OF A RING.

----- FORMER ASSUMED SHAPE.
 ——— REVISED SHAPE.
 FOR $n = 3$

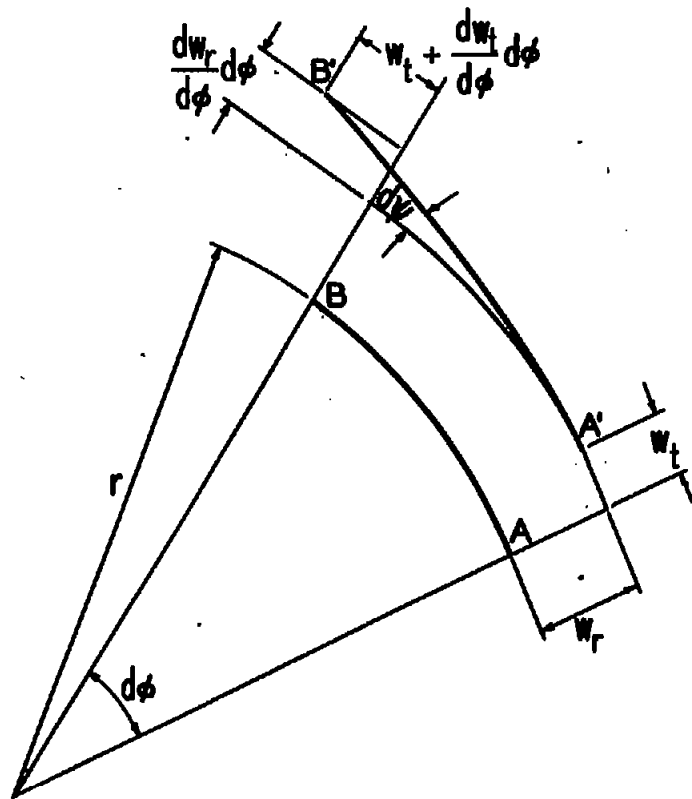


FIG. 2. DEFORMATION OF INFINITESIMAL ARC ELEMENT.

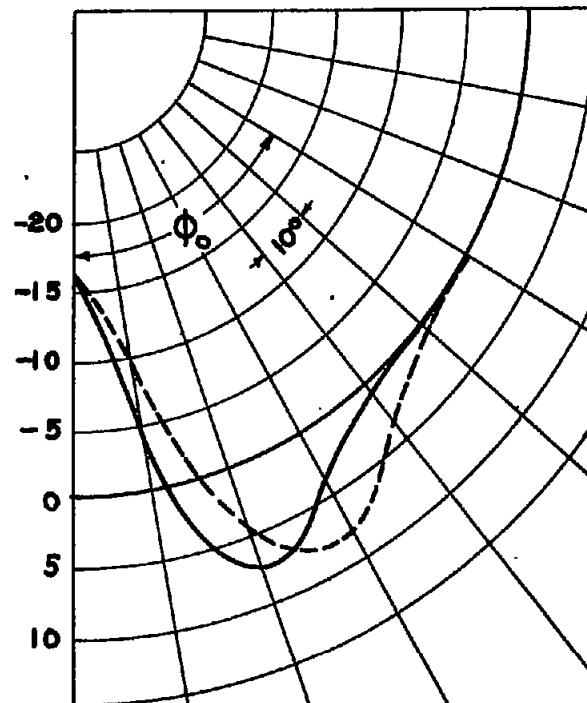


FIG. 3. FURTHER PROPOSED PATTERNS.

----- USING 3 FOURIER COEFFICIENTS.

————— USING 5 FOURIER COEFFICIENTS.

FOR $n = 3$

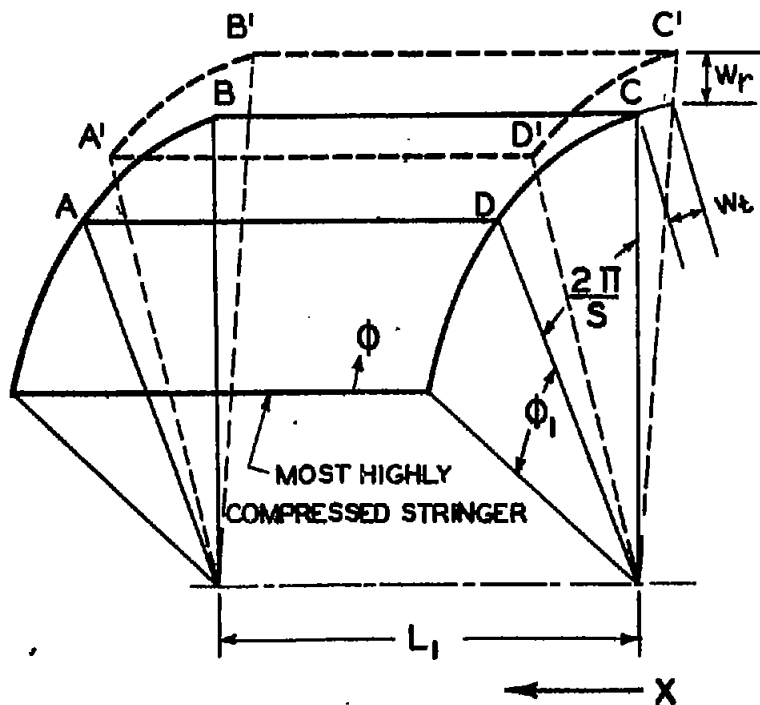


FIG. 4. SHEAR DISTORTION OF PANEL.

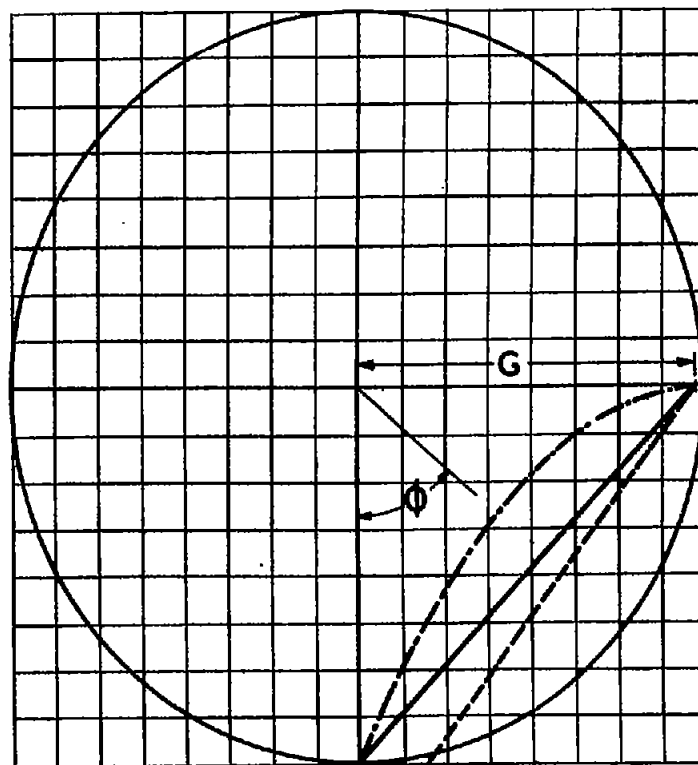


FIG. 5. EFFECTIVE SHEAR RIGIDITY VARIATION.

- $G' = G (1 - \cos \phi)$
- $G' = G (1 - 0.8 \cos \phi)$
- · - · - $G' = G (1 - \sqrt{\cos \phi})$

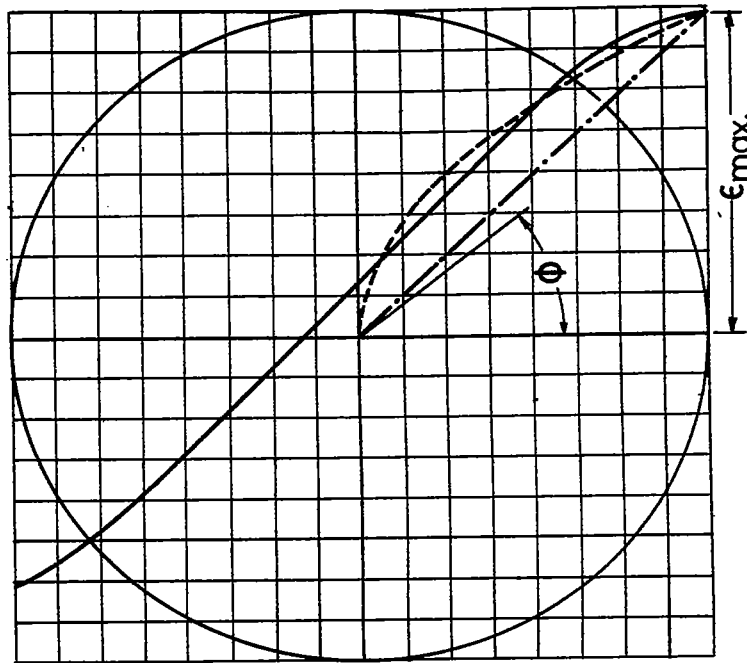


FIG. 6 DIRECT STRAIN DISTRIBUTIONS.
 CALCIT SPECIMEN NO. 159
 PARABOLIC $\epsilon = \epsilon_{max} \sqrt{\cos \phi}$
 LINEAR $\epsilon = \epsilon_{max} \cos \phi$

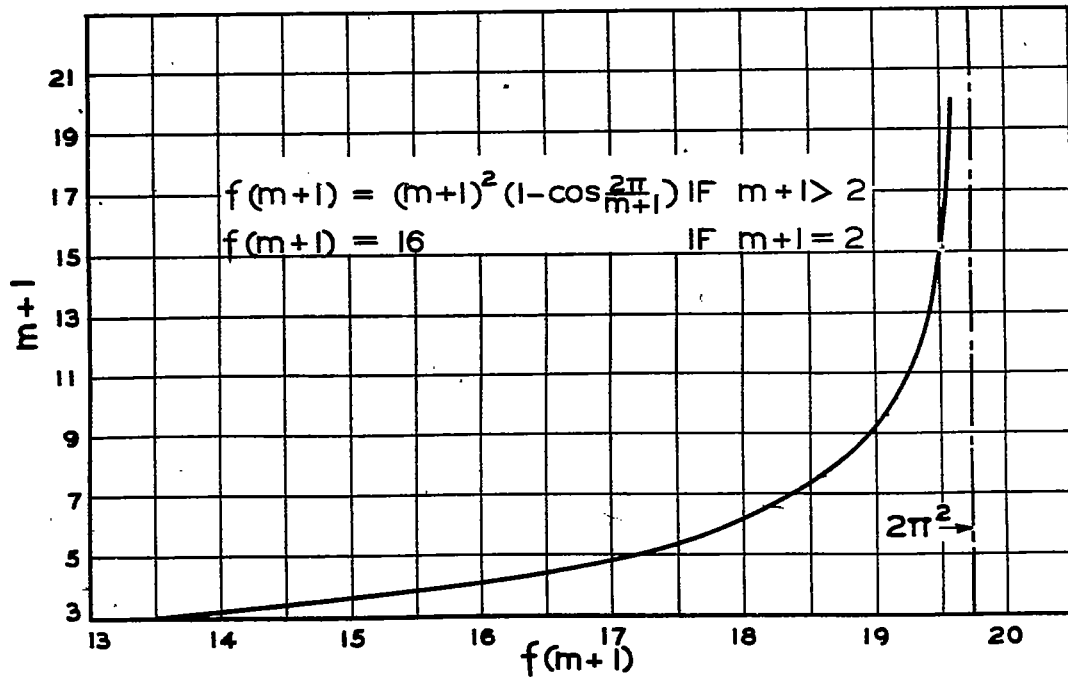


FIG. 7. FUNCTION OF NUMBER OF RING FIELDS INVOLVED IN FAILURE.